INVESTIGATING THE EFFECT OF OIL SATURATION ON ACID PROPAGATION DURING MATRIX ACIDIZATION OF CARBONATE ROCKS

A Thesis

by

RAHUL PRADEEP KUMAR

Submitted to the Office of Graduate and Professional Studies of
Texas A&M University
in partial fulfillment of the requirements for the degree of

MASTER OF SCIENCE

Chair of Committee,	Hisham A. Nasr-El-Din
Committee Members,	Mahmoud El-Halwagi
	Jerome J. Schubert
Head of Department,	A. Daniel Hill

May 2014

Major Subject: Petroleum Engineering

ABSTRACT

The existence of an optimum injection rate for wormhole propagation, and face dissolution at low injection rates during matrix acidizing are well established. However, little has been documented that describes how the presence of residual oil affects carbonate acidizing. This study demonstrates the impact of oil saturation on wormholing characteristics while acidizing field and outcrop cores under reservoir conditions (200°F). Knowledge of the effect of different saturation conditions on acid performance will contribute towards designing more effective acid treatments.

Coreflood experiments at flow rates ranging from 0.5 to 20 cm^3/min were performed to determine the optimum injection rate for wormhole propagation when acidizing homogeneous calcite and dolomite reservoir cores, and low permeability Indiana limestone cores of dimensions 3 and 6 in. length and 1.5 in. diameter. Absolute permeability of the cores ranged from 1 to 78 md. The study involved acidizing cores saturated with water, oil, and waterflood residual oil using 15 wt% HCl. The viscosity of the crude oil used was 3.8 cP at 200°F. CAT scans were used to characterize wormholes through the cores. The concentrations of the dissolved calcium and magnesium ions were measured using Inductively Coupled Plasma–Optical Emission Spectroscopy (ICP-OES) and the effluent samples were titrated to determine the concentration of the acid.

HCl was effective in creating wormholes with minimal branches for cores with residual oil (Sor=0.4-0.5) at injection rates 0.5 to 20 cm^3/min. Compared to brine and oil saturated cores, waterflood residual oil cores took less acid volume to cause breakthrough. Additionally, the wormholing efficiency of regular acid improved with

increases in acid injection rates in the presence of residual oil. A decrease in acid pore volumes to breakthrough for oil saturated cores was noted at high acid injection rates, which could be attributed to viscous fingering of acid through oil. Unlike brine saturated and oil saturated cores, waterflood residual oil cores showed no face dissolution at low acid injection rates. Conclusions from this work aid in the designing of better acid jobs by highlighting the impact of oil saturation on wormholing characteristics of acid while acidizing carbonate rocks.

DEDICATION

I would like to dedicate this thesis to my mom and dad who have stood by me and my dreams. They are the ultimate strength of my life and I would not be what I am today if it was not for their blessings and prayers.

ACKNOWLEDGEMENTS

I would like to thank my committee chair, Dr. Hisham Nasr-El-Din for his support, supervision, and assistance in this thesis. My appreciation also goes to the members of my committee, Dr. Jerome Schubert and Dr. Mahmoud El-Halwagi, for their cooperation and support throughout the course of this research.

I am grateful to my friends – Jia He, Alexis Ortega, Sajjaat Muhemmed Reyath, and Abhishek Punase for helping me with my research and experiments. I appreciate the effort put in by Daniel Shedd to proofread my thesis.

Finally, I would like to acknowledge the financial support of Texas A&M University and the Texas Engineering Experiment Station of Texas A&M University. The facilities and resources provided by the Harold Vance Department of Petroleum Engineering of Texas A&M University are acknowledged.

NOMENCLATURE

PV_{bt}	Pore volumes required to create wormholes along the core length, PV
K_i	Initial permeability, md
S_{or}	Saturation of residual oil

TABLE OF CONTENTS

Page

Page

LIST OF FIGURES

Page

Page

Page

Page

Page

LIST OF TABLES

Page

CHAPTER I

INTRODUCTION AND LITERATURE REVIEW

Carbonate Matrix Acidizing and Wormholing

Matrix acidizing is a well stimulation technique where the acid injected dissolves some of the minerals present in the formation and enhances or increases the permeability around the wellbore vicinity. The whole process can be summarized as an acid-rock interaction with constant alteration to the porous structure of the rock through dissolution. Daccord et al. (1993) showed that the dissolution patterns in carbonates can be classified as uniform, wormhole, or compact, depending on the relative influence of flow rates with respect to the overall reaction rate. Wormholes are larger than the normal pores found in non-vugular carbonates and provide highly conductive flow paths near wellbore.

The patterns and geometry of the wormhole channels formed rely heavily on the rate of mass transfer and the kinetics of the surface reaction (Schechter et al. 1969; and Fredd et al. 1999; Daccord et al. 1989; Wang et al 1993). Compact patterns are formed due to the convection-limited regime at low flow rates. Mass-transport limited kinetics lead to wormhole patterns at intermediate flow rates. Uniform dissolution patterns can be seen at high flow rates where the surface reaction–limited regime dominates.

For regular acid, the patterns developed can be classified as one of the following (Robert and Crowe 2000):

- Compact or face dissolution in which most of the acid is spent near the rock face;
- Conical wormholes;
- Dominant wormholes;
- Ramified wormholes; and
- Uniform dissolution

Wormhole Propagation and Termination

Buijse (2000) and Huang et al. (1997) suggested two possible mechanisms responsible for wormhole termination at the origin. 1) High consumption of acid at the wormhole walls, which limit the acid concentration at the wormhole tip from further propagation. The wormhole tip sees a transformation from mass transfer limited regime to convection limited regime which leads to the extinction of the wormhole. 2) Filtration losses through the wormhole at high flow rates where the surface reaction limited regime predominates over mass transfer limited kinetics.

The effect of acid diffusivity on wormholing was studied by Hoefner and Fogler (1985 and 1987). Matrix acidizing can make wormholes and stimulate up to 10 ft in wells not affected by near-wellbore damage, but if there is damage regular acid cannot propagate the wormhole beyond 3 ft. From coreflood results, microemulsions with low

viscosity and limited mobility of dispersed phase (acid) exhibit acid diffusion rates two orders of magnitude lower than regular aqueous HCl. This means that microemulsions can propagate wormholes in fewer pore volumes than regular acid even under low injection rates where HCl fails. The improved efficiency of acid-in-oil emulsions in propagating wormholes was attributed to reduced diffusion rates in bulk acid solution but could also be a result of reduced fluid loss from the main wormhole. Although Hoefner's work was critical in understanding the contribution of diffusivity of acid through the rock during wormholing, his work ignored an important factor during wormholing, that is, fluid loss which left space for improvement.

Propagation of wormholes depend strongly on fluid losses through the walls of major wormholes (Fredd 2000; Huang et al. 2000; Bernadiner et al. 1992). The efficiency of wormhole propagation is reduced significantly due to acid leaking out and forming highly branched wormholes.

Optimum Injection Rate and Pore Volumes to Breakthrough

Another significant factor in determining the efficiency of the regular acid treatment in creating a single dominant wormhole is the injection rate. Maximum efficiency is attained at an optimum injection rate when the length of the wormhole propagated for the given amount of acid is at the maximum. Researchers have studied the phenomenon of wormhole propagation through different acid-mineral system and established the existence of an optimum injection rate for regular acids (Hoefner and Fogler, 1988;

Daccord et al., 1993; Frick et al., 1994; Mostofizadeh and Economides, 1993; Bazin et al., 1995; Fredd and Fogler, 1998a, 1998b.).

An optimum injection rate for wormhole propagation was determined by calculating the pore volumes to breathrough, PV_{bt}. Fredd and Fogler (1999) studied the dissolution of limestone using DTPA (Diethylenetriaminepentaacetic acid), EDTA (Ethylenediaminetetraacetic acid), acetic acid, and HCl and the pore volumes to breakthrough was determined in each case. Conclusions from their experiments show that at an optimum injection rate a dominant wormhole channel was created and the pore volume to breakthrough was minimum. The number of pore volumes to breakthrough increased for any flow rate less than or greater than the optimum injection rate due to the formation of conical and ramified wormholes, respectively.

The volume of acid required for acidizing can be determined from the wormhole density and its distribution during field operations. Gdanski (1999) proposed a model for carbonate matrix acidizing based on symmetry of wormholing under radial conditions and wormhole density. Wormhole density can be predicted by modeling pressure field around a wormhole (Huang et al. 1999). A combination of the wormhole density model with the wormhole propagation model helps determine the acid volume required to penetrate a given distance.

A semi empirical model to predict the pore volumes to break through and wormhole propagation was developed by Buijse and Glasbergen (2005). The model was based on two experimentally derivable parameters, optimum interstitial velocity and the pore volume to breakthrough corresponding to the same velocity. Both of these parameters

are obtained from coreflood experiments. Furui et al. (2010) designed an integrated flow model by incorporating the tip velocity of acid calculated using the finite element model, into the model developed by Buijse and Glasbergen. However, this model also requires the parameters defined by Buijse and Glasbergen, that is, the optimum interstitial velocity and the corresponding pore volume to breakthrough.

HCl as Acidizing Fluid

HCl has long been used for matrix acidization of carbonates to create wormholes that connect the wellbore to the formation. HCl is inexpensive and there is no precipitation limit to the usage of HCl while acidizing carbonates except when sulphate-rich sea water is used to mix the acid solution, or used in conjunction with acid injection as a preflush, postflush, or spacer fluid, in which cases $CaSO_4$ precipitates, leading to formation damage (He et al. 2011). Since carbonates have a high surface reaction rate, the rate of reaction is mass transfer controlled leading to non-uniform dissolution of carbonates (Economides et al. 2000). Huang et al. (2003) confirmed that at high temperature, HCl produces unacceptable stimulation results because of the rapid reaction near well bore, low penetration and surface dissolution. This means HCl-based fluids have a major drawback when used at high temperatures and low injection rates where they could cause face dissolution. With an increasing flow rate of acid, a larger diameter channel called a conical wormhole is formed (Fredd and Fogler 1998a). Large volumes of acid are consumed for relatively short acid penetration through the matrix, making this mode of wormholing highly inefficient. As injection rate is further increased, the

wormholes become increasingly narrow. The wormhole structure thus formed is most desirable because the acid penetrates the farthest into the formation for the given amount of acid. Williams et al. (1979) suggested maintaining highest possible acid injection rate without fracturing the reservoir rock during the matrix acidization of carbonates but at higher acid injection rates, the wormhole structure becomes highly branched and consumes increasing volumes of acid as the wormhole propagates through the carbonate matrix. Eventually, at sufficiently high acid injection rates, the fracture pressure is exceeded and the acid forms a fracture instead of a wormhole.

Effect of Oil Saturation While Acidizing Carbonate Rocks

Coreflood experiments provide representative data that are scaled up to the reservoir size and magnitude. However, these experiments are conducted on clean rock samples because it is assumed that the preflush will displace all formation fluid out of the target zone, preconditioning it for the main acid stage. Thus, the rocks do not always represent the actual formation conditions. During matrix acidization, the saturation conditions of the near-wellbore area affected by acid at the beginning of acid injection varies significantly for both oil and gas wells. Any saturation condition is possible. Some saturation conditions for oil wells are as follows (Shukla et al. 2006)-

- The near-well vicinity is flushed with drilling and/or completion-fluid filtrate upon initial completion during acid treatment. Upon injection of water-based drilling fluids, the near-well vicinity would change saturation conditions to water and oil saturated, with oil present at residual oil saturation. However if

oil based fluids were used for completion, the near-well vicinity would be oil saturated with water present at connate or irreducible saturation.

- A new phase saturation is created during the pre-flush stage of an acid treatment if any fluid other the normal produced fluid is injected into the formation ahead of acid. For instance during preflush of brine (as a kill fluid) ahead of acid injection, results in the near-well vicinity having high water saturation when acid enters the formation.
- In oil producing wells, after a certain period of oil production, the near-well vicinity would be primarily oil saturated with water present at irreducible water saturation. Of the many variations possible to this state, one possible condition is when the well is producing water. Here, while certain regions may have intermediate levels of water and oil saturation, others intervals could have high or low water saturations. Oil is likely to be at residual level in regions with high water saturation.

One of the methods of secondary oil recovery is waterflooding, where water from the injection well physically sweeps the displaced oil to the producing well. The oil present here is likely to be at residual saturation. The wormholing process would involve a two-phase fluid system in the presence of hydrocarbon or gas. Thus, the process gets more complicated, especially when the rock is pre-saturated with hydrocarbon.

However, this system must not be confused with the pumping of a two-phase acid system such as emulsified acid or foamed acid. In an emulsified acid system the internal phase used is usually HCl and the external phase is a hydrocarbon such as diesel, which

acts as a diffusion barrier between acid and rock (Crowe et al. 1974; Bergstrom et al. 1975; Hoefner et al. 1985; Daccord et al 1989). The diffusion barrier created reduces the acid-rock reaction rate, which, in turn, results in deeper penetration of live acid into the formation, thus enhancing the effectiveness of emulsified acid in creating wormholes (Willams et al. 1972; Guidry et al. 1989; Navarrete et al. 1998a and b). Apart from the slow reaction rates, these acid systems have relatively high viscosity. This ensures improved sweep efficiency through better distribution of acid in the formation (Buijse and Van Domelen 2000).

Peters et al. (1989) tried introducing a second internal phase in the form of gaseous nitrogen which would compete with HCl and retard its release. This ensured lower acid reactivity and availability for propagating deeper wormholes. Foamed acid provides better leakoff control during acid fracturing (Foshee and Hurst 1965) and efficient wormholing during matrix acidization. (Bernadiner et al. 1992).

Although emulsified acid is a better stimulating fluid at low injection rates because of deeper penetration and the absence of compact or face dissolution, plain HCl gives better results at higher flow rates (Bazin and Abdulahad 1999).

Mahmoud et al. (2011) evaluated the effect of water, oil, and gas while acidizing calcite cores using 0.6M concentration of GLDA, HEDTA, and EDTA at a pH of 4 and a temperature of 300°F. Experimental results indicated improved performance of chelating agents in the presence of residual oil. The authors also noted the absence of face dissolution at low GLDA injection rates and high temperatures.

Sayed et al. (2012) studied the effect of the presence of crude oil in the formation on the performance of emulsified acid in stimulating carbonate formations. Emulsified diesel was mixed with 36.8 wt% HCl, de-ionized water, and corrosion inhibitor to prepare the acid solution which was used to treat acidized high permeability Indiana limestone cores. Their work indicated enhancement in rock permeability after injecting emulsified acid through water saturated cores at high flow rates. Emulsified acid took greater pore volumes to cause breakthrough in cores saturated in oil and water as compared to cores saturated only in water. However, a clear relationship between injection rate and acid volume required to propagate wormhole through crude oil and water saturated cores could not be proven.

Shukla et al. (2006) evaluated the effects of oil on wormholing process by coreflood experiments on Texas Cream Chalk cores with dimensions of 6 in. length and 1 in. diameter using 15 wt% HCl. The oil in the cores was replaced with brine before acid injection. Pore volume for acid breakthrough of these cores was similar to cores saturated in brine. However, when gas was injected before the acid, the pore volume to breakthrough decreased by an order of 1/2 to 1/3 less than when acid was injected without gas. Thus, ensuring high saturation of the immiscible phase when acid enters the matrix ensures better stimulation during matrix acidization of carbonates. It is interesting to note that these experiments were conducted at room temperature and might not apply to reservoir conditions.

The presence of an immiscible phase can reduce fluid loss from the main wormhole and create deeper penetration by reducing the relative permeability to the acid in the

matrix surrounding the wormhole. This is accomplished by avoiding an aqueous preflush in low-water-cut oil-production wells. In the case of the water producing wells, or in injection wells, the wormholes can be better propagated by injecting gas or oil before the acid.

The effect of residual oil on wormhole propagation is rate dependant for gelled and in-situ gelled acid (Gomma and Nasr El-Din 2011). Experimental results from acidization of Indiana Limestone cores of a length of 6 in. and a diameter of 1.5 in. at 200°F indicated that Fe(III) cross linkers used in HCl formulations induced sludge which in turn lead to formation damage. During the pre-flush stage, the oil left behind in the core increased with increasing water injection rate. At any injection rate, HCl required a greater pore volume to cause breakthrough in cores with residual oil as compared to gelled acid or in-situ gelled acid. At acid injection rate of 2.5 cm^3/min, damage due to gel was reported to be less in the core that had no oil. However, at an injection rate of 10 cm^3/min the final pressure drop across the core without oil was higher than the core with oil. This indicated the damage due to the gel was more severe in clean cores over cores with residual oil. The authors claim that an injection rate of 10 cm^3/min is the transitional point at which damage due to the gel was reduced in cores with residual oil. Nevertheless, their conclusions remain questionable because they were drawn from experiments run at just two flow rates and do not necessarily indicate a trend or transitional behavior. In addition, the authors did not indicate whether the effective pore volume (volume of the pore excluding the volume occupied by oil) was considered while calculating the pore volume to breakthrough.

Al-Mutairi et al. (2012) studied the wormholing effect and characteristics of regular acid (20 wt%) and emulsified acid on cores saturated with 5 wt% KCl, crudes of varying API° gravities, and tar during matrix acidization of carbonates. Reservoir cores of 1.3 to 1.7 in. in length and 1.5 in. diameter were used. Experimental results at 200°F indicated that formations with tar exhibited no face dissolution, even at low flow rates, because tar acted as a barrier to the reactivity of acid with the rock. Both the regular acid and the emulsified acid showed comparable wormhole penetration for tar bearing formations. The beneficial effects of emulsified acid were reduced significantly when oil saturated the rocks. The reason was attributed to the fact that regular acid droplets diffused faster and diluted more, thus providing a similar magnitude of retardation as emulsified acid. Lighter oil (°API of 45) allowed better diffusion of acid droplets to the rock surface as compared to intermediate oil (°API of 32), reducing the acid pore volume to breakthrough. Thus, knowledge of the type of oil saturating the core is crucial when selecting the acid for treatment. The authors also noted that clean and tar bearing plugs did not show a clear difference in wormholing efficiency when regular acid was used. However, their explanation of the phenomenon of the oil coating the pore surfaces remaining unavailable for pickup by acid to form emulsions remains unsubstantiated.

Research in carbonate acidizing has progressed a long way from pore scale to field scale. Investigators have studied in detail how pores enlarge and develop into wormholes which expand and propagate through cores. Much has been published to date explaining the kinetics behind the diffusion and convection combined with mass transport of acid propagating the wormhole. A plethora of theoretical models has been developed to

provide quantitative results comparable with the corresponding experimental work while identifying the optimum acid flux. While most of these models have established the existence of an optimum injection rate and accounted for the factors affecting this rate, little has been documented that explains the effects of residual crude oil on wormholing characteristics of the acidizing fluid in cores under reservoir conditions.

Literature survey shows contrasting results as to how residual oil affects pore volume to breakthrough. Gomaa et al. (2011) showed that as flow rate increased, higher pore volumes of regular acid were required to break through cores with residual oil saturation. Shukla et al. (2006) claims that residual oil saturations in carbonate cores had little effect on the acidizing process and that these cores have the same wormholing effect as cores completely saturated with water. Al-Mutairi et al. (2012) accounted for the lower acid pore volume to breakthrough in the presence of lighter oil as a result of formation of in-situ acid in oil emulsion, which aided formation of deeper wormholes.

However, many of these investigations were conducted at room temperature and pressure and do not replicate actual reservoir conditions. Many of the conclusions were drawn from as few as two experimental runs, which do not necessarily indicate a trend. In addition, some of the authors have based their results on theoretical assumptions, leaving without substantiating their theories with experimental data.

CHAPTER II

EXPERIMENTAL SET-UP AND PROCEDURE

Materials

Field cores from carbonate reservoirs in the Middle East and Indiana Limestone cores were used in all experiments. Permeability of the cores used for determining optimum injection rate of water-saturated cores, oil-saturated cores and waterflood residual oil cores varied from 1 to 78 md. The dimensions of the cores and acid injection rates chosen for running coreflood experiments have been furnished in **Table 1**.

Fluid Properties

The density and viscosity of 5 wt% KCl brine prepared was found to be 1.0315 g/cm^3 and 1.077 cp at room temperature and pressure. The naphthenic crude oil used to bring the cores to residual oil saturation had a measured density of roughly 28°API at 77°F and 41°API at 200°F. The viscosity of the same crude oil used was measured to be 32.2 cP at 77°F and 3.8 cP at 200°F.

Fluid Preparation

The acid solution was prepared using deionized water obtained from a water purification system that has a resistivity of 18.2MΩ.cm at room temperature. The concentration of the hydrochloric acid used for this experiment was 36.8 wt%. This acid was diluted to 15 wt% using deionized water.

TABLE 1-COREFLOOD STUDY

Cores Saturated In Deionized Water				
Exp No #	Core Diameter ×Length, in.	K_i, Initial Permeability**, md	Injection Rate, cm^3/min	PV_{bt}
1	1.49 * 3.53	5.0	0.5	9.5
2	1.49 * 2.94	1.2	2	5
3	1.48 * 3.03	6.1	5	1.81
4	1.45 * 3.32	6.1	10	1.14
5	1.49 * 2.60	6.5	20	1.39

Brine Saturated Cores with Residual Oil					
Exp No #	Core Diameter× length, in.	K_i, Initial Permeability*, md	Permeability with residual oil, md	Injection Rate, cm^3/min	PV_{bt}
6	1.49*2.97	77.9	21	0.5	1.1
7	1.49*2.57	15.5	3.9	1	0.83
8	1.48*2.68	17.7	4.2	5	0.68
9	1.40*3.04	24.3	3.8	10	0.67
10	1.49*2.45	56.2	25	20	0.61

Cores Saturated in Crude Oil				
Exp No #	Core Diameter× length, in.	K_i, Initial Permeability**, md	Injection Rate, cm^3/min	PV_{bt}
11	1.5*3	3.9	1	4.41
12	1.5*3	6.7	5	3.90
13	1.5*3	6.7	10	5.10
14	1.5*3	3.7	20	3.91

Cores under various saturation				
Exp No #	Core Diameter × Length, in.	K_i, Initial Permeability*, md	Injection Rate, cm^3/min	PV_{bt}
15 (brine saturated)	1.5*6	4.3	0.5	4.46
16(fully saturated in oil)	1.5*6	-	0.5	1.49
17 (residual oil saturated	1.5*6	1.3	0.5	0.68

* - Initial permeability was measured under vacuum-brine saturation
** - Initial permeability was measured under vacuum-deionized water saturation

The corrosion inhibitor used is a quaternary amino-based compound (CI-25) added to the acid solution to prevent corrosion of the accumulators and lines. The formulation of the corrosion inhibitor has been patented by BJ services. The acid solution was prepared by mixing de-ionized water, corrosion inhibiter, and hydrochloric acid for 30 minutes.

Preparation of Cores

The cores used for water-saturated and waterflood-residual-oil experiments were received from carbonate reservoirs in the Middle East. A Dean Stark apparatus was used to remove any fluid present in these cores before they were saturated in different fluids.

These cores were split into two categories. One half of the cores were saturated in de-ionized water and the other half in 5 wt% KCl. The cores were saturated in water using a vacuum saturation pump and were left in deionized-water until acidizing.

The remaining cores were saturated in KCl using a vacuum saturation pump and were flushed with at least 4 pore volumes of crude oil to bring the brine saturation in the cores to irreducible levels (S_{wir}). These cores were then flushed with at least 4 pore volumes of 5 wt% KCl brine to reduce the oil in core plugs to residual saturation (S_{or}). Finally, the cores with residual crude oil were preserved in 5 wt% KCl until acidization.

The third set of coreflood experiments were conducted on Indiana Limestone cores fully saturated in oil. These cores were prepared by drying the core in an oven at 450°F for at least 24 hours to remove any moisture. The cores were then saturated in naphthenic crude oil by pumping atleast 4 pore volumes of oil through the cores at

extremely low flow rates over a period of 24 hours. This ensured complete saturation of core in crude oil.

Compatibility Test

Compatibility tests between crude oil and acid were conducted at 200°F. Nothing was added to the acid system apart from the corrosion inhibitor used to prepare the acid for the coreflood study. Equal volumes of acid and crude oil were mixed followed by centrifugation at 3000 rpm for 10mins. This was done to check the extent of emulsification of acid or formation of precipitation upon the mixing of acid and oil. From **Fig. 1,** a clear oil-acid contact layer was observed with no emulsion or precipitation formed.

Fig. 1—Compatibility test between Naphthenic crude oil and HCl acid system

Coreflood Setup

The coreflood setup used to simulate the matrix acidizing process has been described in **Fig. 2.** The experimental setup consists of two accumulators, syringe pump, core holder, back pressure regulator, hydraulic pump, fraction collector, differential pressure transducer, and a data acquisition system. A heating system is used to heat the core in the core holder.

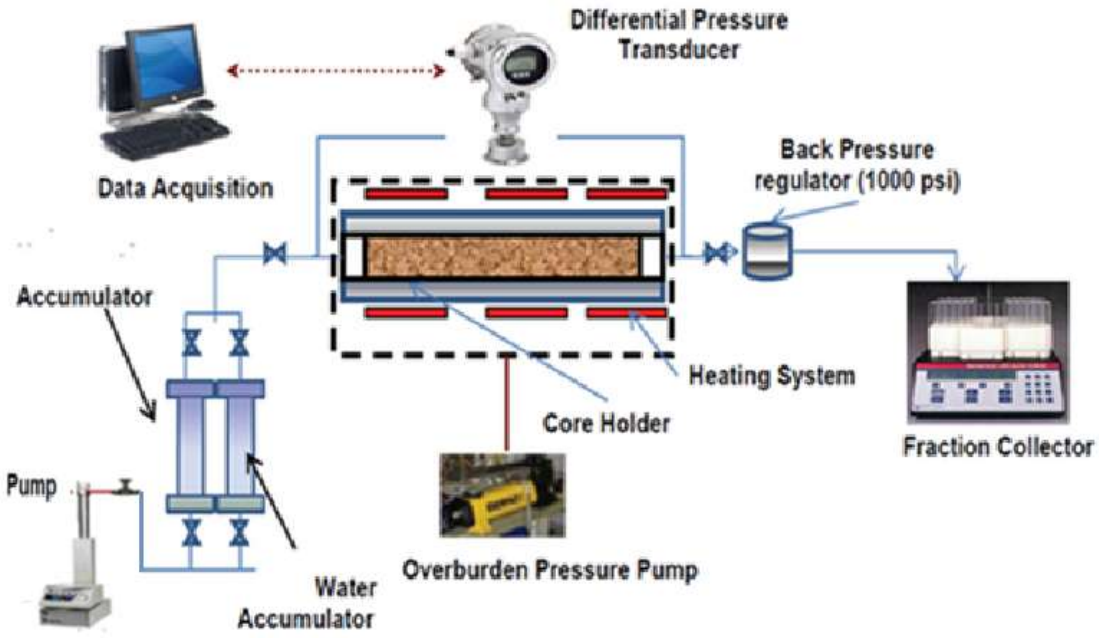

Fig. 2—Coreflood setup

Accumulators

One of the accumulators used in the experiment was used to store brine/deionized-water and the other stored acid. The accumulator consists of a teflon piston which splits the unit into two compartments, one side filled with hydraulic oil and the other compartment filled with brine/deionized water/acid. When the experimental setup is

complete, the syringe pump removes hydraulic oil from the reservoir and pushes it up into the oil compartment. The hydraulic oil in turn moves the piston up, which pushes the brine/acid/de-ionized water out of the accumulator and into the lines connected to the core holder. A special Nickel-Chromium-Molybdenum wrought alloy, Hastelloy C-276, was used to make the acid accumulator with a capacity of 1,000 ml. The brine/deionized water accumulator, made of stainless steel, has a capacity of 2,000 ml.

Core Holder

The core holder is a metallic cylinder where the core is held under a confining pressure called the overburden pressure. Generally, an overburden pressure of 1500 psi was maintained throughout all the experiments. The confining pressure is required to be at least 400 psi greater than the core inlet pressure. The core holder is made of Hastelloy C-276, which contains tungsten in addition to the regular Nickel-Chromium-Molybdenum alloy for improved corrosion resistance. The core holder is capable of withstanding pressures up to 3000 psi and temperature as high as 300°F. A rubber sleeve within the core holder prevents direct contact between the core and the metallic-alloy cylinder.

Syringe Pump

A Teledyne ISCO D500 precision syringe pump with a capacity of 507 ml and a maximum allowable working pressure of 2,000 psi, was used to inject the hydrochloric

acid solution into the core. The pump is used to set a constant flow rate ranging from 0.1 ml/min to 400 ml/min. The specification of the pump is shown in **Table 2.**

TABLE 2–SYRINGE PUMP SPECIFICATION (TELEDYNE ISCO, INC., 2013)	
Capacity:	507 ml
Flow Range (ml/min):	0. 001 - 204
Flow Accuracy:	0.5% of setpoint
Displacement Resolution:	31.71 nl
Motor Stability:	± 0.001% per year
Pressure Range (psi):	10 - 3,750
Standard Pressure Accuracy:	0.5% FS
Optional Pressure Accuracy:	0.1% FS
Wetted Materials (standard):	Nitronic 50, PTFE, Hastelloy C-276
Plumbing Ports:	1/8" NPT
Operating Temperature:	5 - 40° C Ambient
Power required:	100 Vac, 117 Vac, 234 Vac, 50/60 Hz (specify)
Dimensions (HxWxD, cm):	103 x 27 x 45
Weight:	Pump module - 33 kg; controller - 3 kg
Standards conformity:	EN1010-1, EN61326-1998, UL6101A-1, CSA1010

Back Pressure Regulator

The downstream pressure at the end of the core holder is regulated using a back pressure regulator. The pressure is maintained at about 1,100 psi throughout the acidizing experiment in order to keep the CO_2 produced from the dissolution of carbonates in solution without affecting the system hydrodynamics (Lund et al. 1973; Fredd and Fogler, 1998c). The back pressure setup helps simulate the actual reservoir conditions wherein under static conditions, the pressure inside the core equals reservoir pressure.

Hydraulic Pump

The confining pressure within the core holder is provided using a hydraulic pump which can supply pressure up to 10,000 psi. The hydraulic pump is a product of Enerpac Co., model P-39 with a usable oil capacity of 770 cm^3.

Data Acquisition System

The data acquisition system consists of a pressure transducer which monitors the pressure drop across the core. It relays the pressure drop to a signal processing board which in turn delivers the processed signal to the computer where the Labview software records the pressure drop at regular intervals. Foxboro model IDP10 I/A series differential pressure transmitters were used record the pressure drop across the cores. An Inductively Coupled Plasma – Optical Emission Spectrometer (ICP-OES, Optima 7000DV) was used to determine the calcium ion concentration in the effluent samples.

The effluent samples were titrated using a Thermo Scientific Orion 950 Titrator to determine the concentration of acid.

Fraction Collector

The effluent samples during acidization of the core sample were collected at regular intervals in 15 ml tubes using a Spectra/Chrom® CF-1 Fraction Collector. It can collect upto 174 fractions where each fraction size is pre-set in terms of either time or drop collected.

Inductivity Coupled Plasma – Optical Emission Spectrometer (ICP-OES)

The effluent samples from the core flood experiments were analyzed using ICP-OES analysis to detect the presence of metal ions – calcium and magnesium. ICP-OES, Optima 7000DV is an emission spectrometer from Perkin Elmer. It works on the principle of detecting elements based on electromagnetic radiations from excited atoms and ions produced by the inductively coupled plasma (Perkin Elmers Inc.,2013). The effluents samples from the coreflood were diluted 1000 times using deionized water of 18.2-MΩ.cm resistivity at room temperature to bring the concentrations of the samples within detectable range of the instrument. Calcium and magnesium concentrations were processed and reported by software named WinLab32 based on the calibration curves created from standard solutions of known concentrations. Results within an accuracy range of ±5% can be obtained depending on the calibration quality of the system.

Acid Titrator

The effluent samples were titrated using a Thermo Scientific Orion 950 Titrator to determine the concentration of acid. 0.1M and 1 M NaOH base solutions were used to titrate the acid in the effluent samples. The specifications of the titrator are shown in the **Table 3.**

TABLE 3—THERMO SCIENTIFIC ORION 950 TITRATOR SPECIFICATIONS (COLE-PARMER, 2013)	
Product Type	Potentiometric titrators
Temp accuracy	±0.1
mV range	±1600
mV resolution	0.01
Temp range	-5 to 105°C
Display	LCD
Dimensions	Meter: 9 in W x 2 in H x 7.5 in D Dispenser: 5.5 in W x 16 in H x 18 in D
Power (VAC)	110/120
CE Compliance	Yes
Output	RS-232
Power (Hz)	50/60
Brand	Thermo Scientific Orion
Manufacturer number	095000
Model	095000

Computer Assisted Tomography Scan (CT scan)

The core plugs used in the experiments were cut from carbonate reservoirs in the Middle East and Indiana Limestone cores. The cores were subjected to CT scan in order to determine the CT number of the core. CT number served the primary source of identifying the extent of dolomitization, presence of anhydrites, and porosity. Porosity of a core after treatment can be determined from the CT number (Izeg and Demiral 2005). The following equation is used to determine porosity from CT number:

$$\emptyset = \frac{(CT_{wr} - CT_{ar})}{(CT_w - CT_a)} \quad \text{.....(1)}$$

Where:

CT_{wr} = CT number of water saturated rock, CT_{ar} = CT number of air saturated rock,

CT_w = CT number of water, = 0, CT_a = CT number of air, = -1000.

Good porosity or presence of a fracture is indicated by a CT number of 2,200 or less (Nevans et al. 1996). CT number of about 2,350 and 2,250 indicates the presence of pure dolomite and pure limestone respectively. The presence of extensive anhydrite is confirmed by a CT number of 2,550 or higher. The cores were scanned and imaging software named ImageJ® was used to analyze and stack the images in a single window. The software is designed to compile the images of cores taken over different cuts along the length of the core as shown in **Fig. 3.**

Based on the images obtained from the CT scan and the CT number, the cores were broadly divided under the following descriptions: carbonates with streaks of anhydrite, carbonates with vugs and anhydrite, carbonates with traces of anhydrite, and pure limestone. The lighter shades in the CT images indicate the presence of high density

minerals like anhydrites while darker shades indicate low density caused by the presence of vugs or wormholes. Homogeneous cores without vugs were chosen for the coreflood experiments.

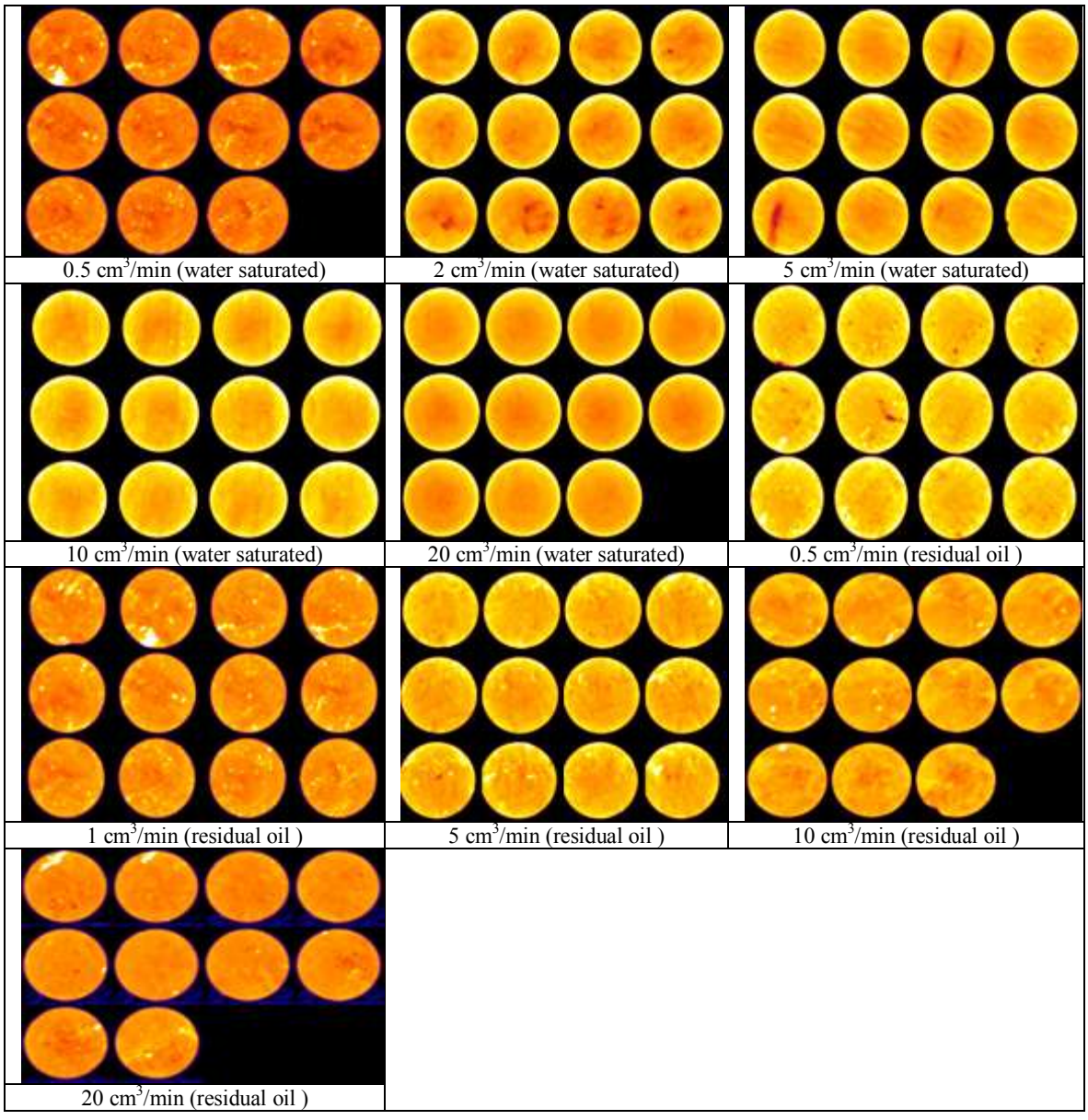

Fig. 3─CAT scan images of the field cores before injection of acid. The lighter shades in the CT images indicate the presence of anhydrites.

Scanning Electron Microscope (SEM)

Scanning electron microscope (SEM) is an electron microscope that produces images of the sample by focusing a high-energy beam of electrons on the sample and combining the position of the beam with the detected signal to produce the image. A raster scan pattern is used to scan the high-energy beam of electrons. The signals produced by the interaction of these electrons with the atoms of the sample contain information about the sample's composition, topography, and electrical conductivity. SEM analysis was performed for representative samples to determine the composition of the core. These results were compared with the results from CAT scan to confirm the lithology of the cores. While all the cores show the presence of calcium, carbon, and oxygen, only some showed traces of magnesium. Although the CT scan images indicated presence of anhydrite, the SEM analysis didn't detect any sulphur in the samples, possibly because of the presence of only trace amounts of anhydrite in the cores. **Table 4** gives a brief summary of the SEM analysis of selected-representative field cores.

TABLE 4—SUMMARY OF SEM ANALYSIS OF CORE SAMPLES

Exp #	Element (wt %)				
	O	Ca	C	Mg	S
4	48.95	39.78	11.27	-	-
6	51.46	36.64	11.10	-	-
7	55.43	30.45	14.12	-	-
9	54.28	37	8.61	-	-
10	33.18	47.91	10.9	7.51	-

CHAPTER III

COREFLOOD STUDY ON WATER SATURATED CORES

Acidizing experiments with the hydrochloric acid system were run using the coreflood setup shown in **Fig. 2**. **Table 1** summarizes all the data from the coreflood study of cores saturated in deionized water. The cores saturated in deionized water were loaded into the core holder and an overburden and back pressures were applied. Coreflood runs were performed using 15 wt% HCl at injection rates of 0.5, 2, 5, 10, 20 cm^3/min. All the core flood experiments were performed at 200°F. The cores were flushed with de-ionized water until the system achieved desired temperature of 200°F. The pressure drop across the cores was plotted using the Lab View software. The coreflood test was terminated when a constant pressure drop was achieved. The effluent samples were collected using the automated fraction collector and the calcium concentration in the samples was measured. The pH value and the density of the effluent samples were measured. The acid concentration in the effluent samples was also measured. Following the coreflood experiments, the propagation of the wormhole through the cores were analyzed using CT scan technique.

Coreflood Study

Pressure drop across the core during the injection of regular acid at an injection rate of 0.5cm^3/min and 200°F is shown in **Fig. 4**. Although the pressure drop across the core stabilized at 23 psi during water injection, an initial rise in pressure drop was noticed the

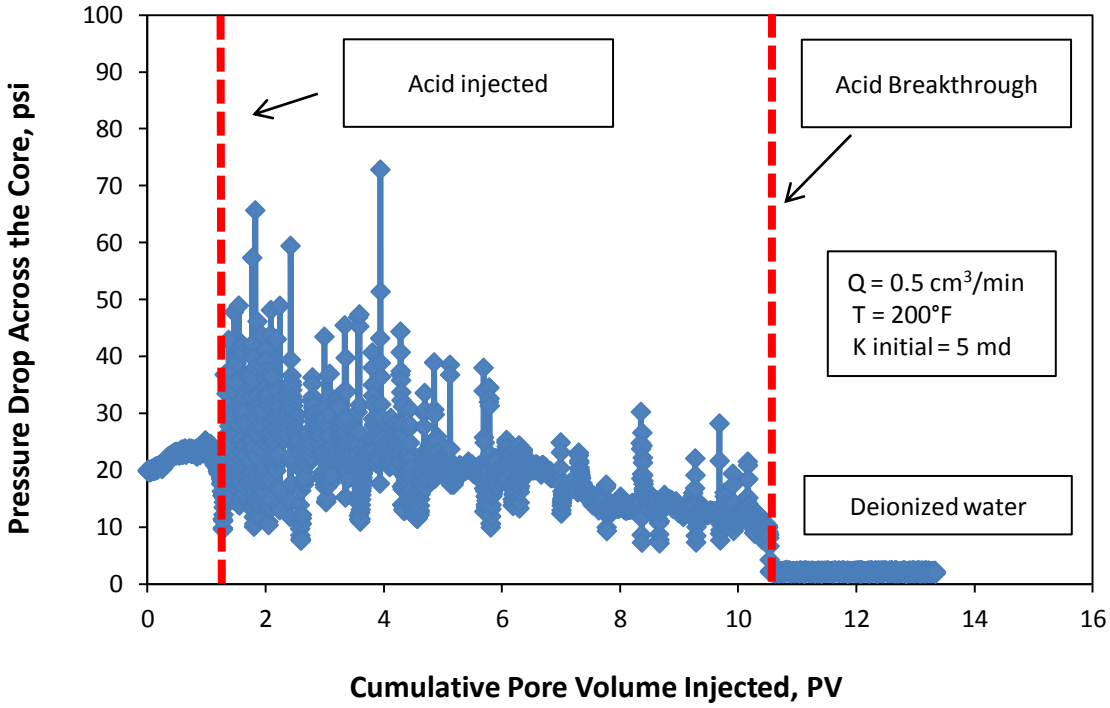

Fig. 4—Pressure drop across the core at an acid injection rate of 0.5 cm^3/min and 200°F.

instant acid was injected. This is because of the sudden rise in viscosity of the fluids flowing through the lines when deionized water was switched with the acid. The pressure drop increased until acid found a region of least resistance and highest permeability within the core and changed its direction of flow within the core. This behavior continued as the acid propagated through the core. The cycling trend of the pressure drop that follows the injection of acid at 0.5 cm^3/min is because of CO_2 release. Although a back pressure of 1,100 psi was maintained, a portion of the core was dissolved in acid, which released CO_2 from solution. 9.5 pore volumes of acid were injected until the pressure drop fell from 11.45 psi to of 2.11 psi. The drop in pressure

indicated acid breakthrough. Upon acid breakthrough acid injection was stopped and de-ionized water was injected as a post flush.

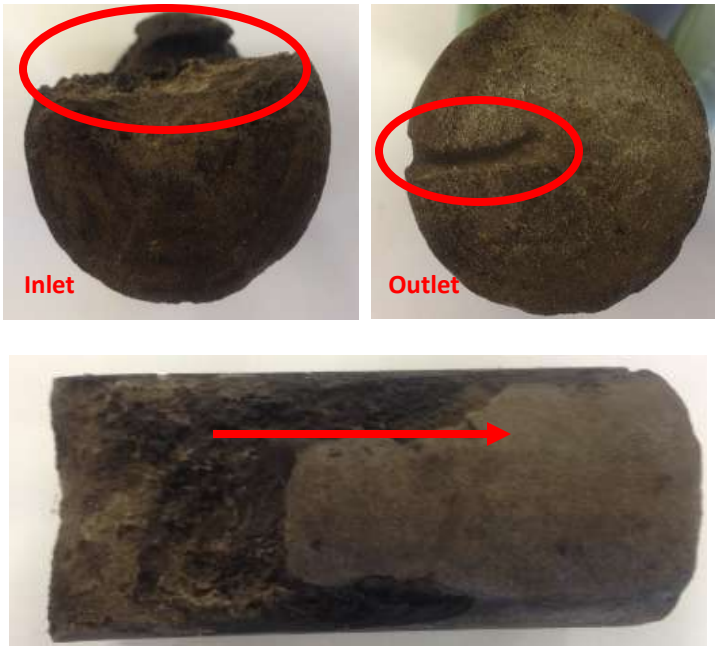

Fig. 5—Acid face dissolution of water saturated cores at 0.5 cm^3/min and 200°F

Fig. 5 shows washout across the cross section of the core because of high leakoff rate which accounted for higher pore volume for breakthrough. The pore volume to break through the core at 0.5 cm^3/min was found to be as high as 9.5. As HCl reacted with the carbonate plug, the pressure drop decreased gradually because of the wormholes formed. This was marked by the rise in calcium and magnesium concentration in the effluent fluid. The wormholes penetrated along the length of the core until acid breakthrough occurred. The acid concentration in effluent samples at 0.5 cm^3/min was

profiled as shown in **Fig. 5**. The highest effluent acid concentration marks the point of acid breakthrough.

Most of the effluent samples in the beginning of acid injection measured near zero acid concentration because all the acid injected was utilized in creating and propagating the wormhole. Once the wormhole was formed and acid broke through, the partially reacted acid made its way through the core and reached the core outlet. The concentration of the acid in the effluent sample at acid breakthrough had reduced from 15 wt% HCl to 9.16 wt% upon reaction with the calcite rock.

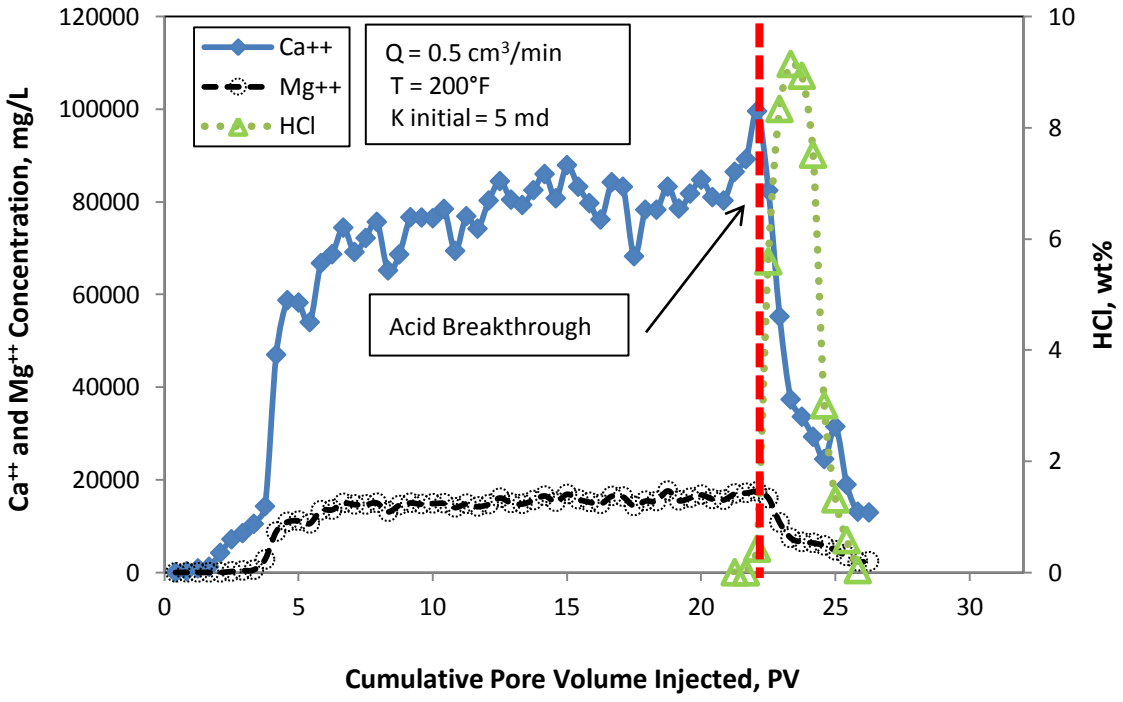

Fig. 6-Calcium, magnesium, and HCl concentrations in the effluent samples at acid injection rate of 0.5 cm^3/min.

The calcium and magnesium concentration in the effluent samples for the same experiment is represented in **Fig. 6.** Calcium and magnesium concentrations were close to zero at the start of water injection, then increased gradually after acid was injected, and decreased again once injection of water started. The calcium concentration in the effluent acid reached as high as 99,600 mg/L. The highest magnesium concentration was found to be 17,638 mg/L. The effect of injection rate on wormhole propagation was examined by running coreflood experiments at flow rates of 2, 5, 10, and 20 cm^3/min.

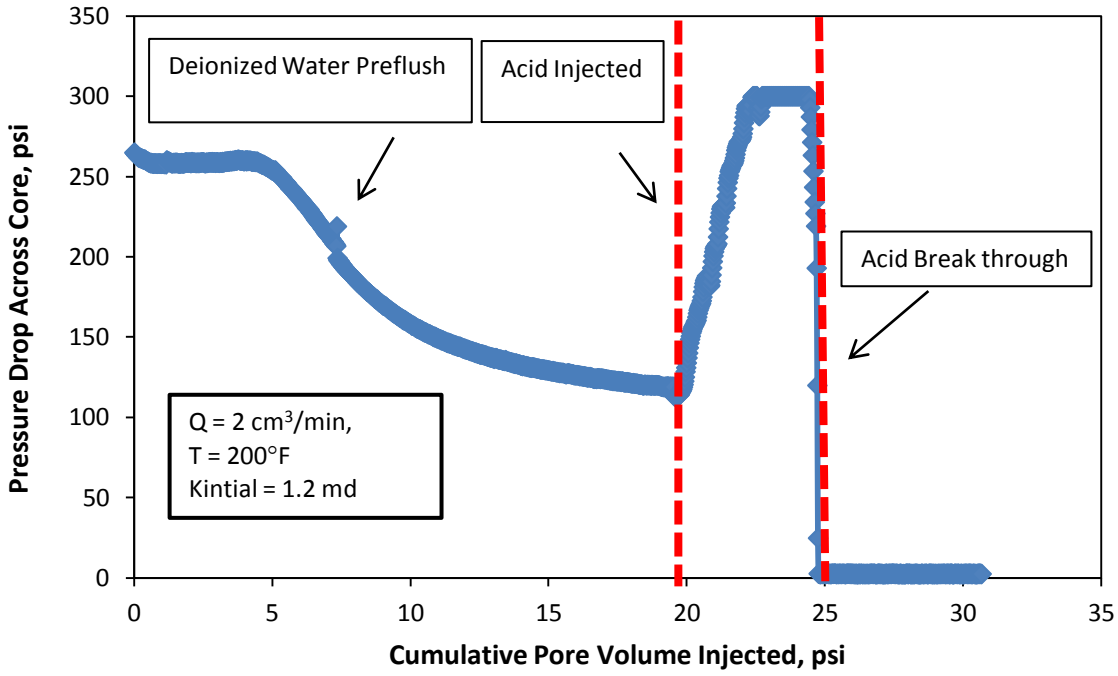

Fig. 7-Pressure drop across the water saturated core at an acid injection rate of 2 cm^3/min and 200°F.

At an injection rate of 2 cm^3/min the pressure drop stabilized at around 122 psi during water injection. After reaching a stable pressure drop, acid was injected, leading to an initial rise in pressure drop because of a change in viscosity of the fluid flowing through flow lines followed by sharp dip in pressure as HCl broke through the core. 5 pore volumes of acid were required for break through. Pressure drop across the core during injection of regular acid at 2 cm^3/min and 200°F is shown in **Fig. 7**. The pressure drop across the cores rose as high as 300 psi before breakthrough because the core had low initial permeability (1.2 md).

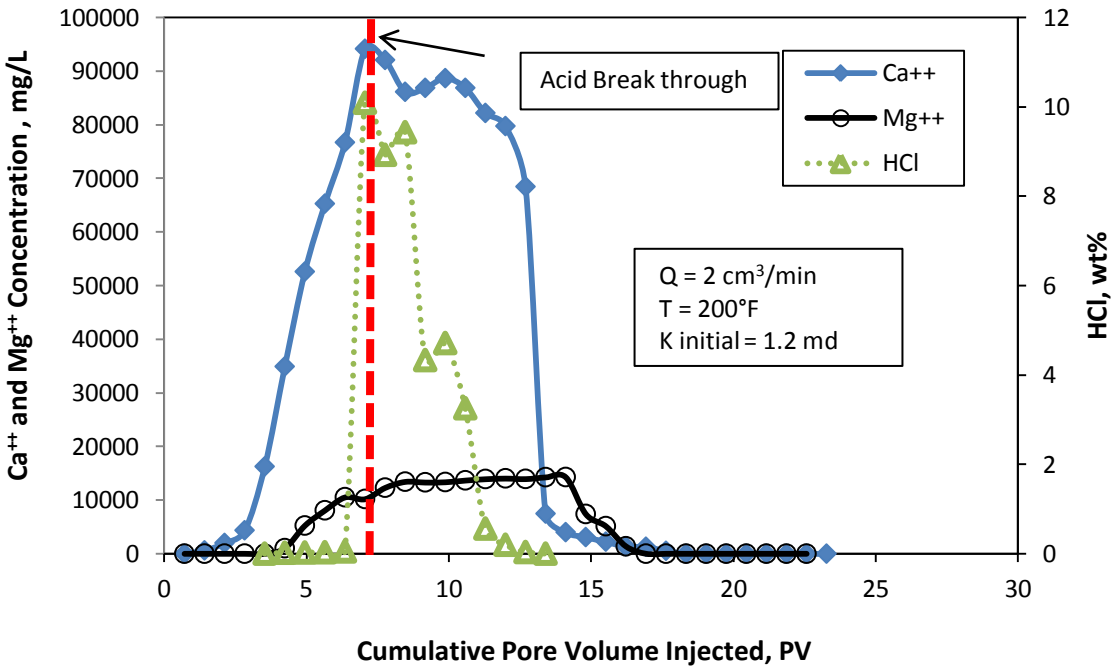

Fig. 8-Calcium, magnesium, and HCl concentrations in the effluent samples at acid injection rate of 2 cm^3/min.

It was interesting to note that there was face dissolution observed at 2 cm^3/min too, however, it was not as prominent as the one observed at 0.5 cm^3/min. This also justifies the fact that the acid took less pore volume to breakthrough at 2 cm^3/min as compared to 0.5 cm^3/min.

The calcium and magnesium concentration in the effluent samples measured 94,170 mg/L and 14,270 mg/L respectively at acid breakthrough. Again, face dissolution accounts for the high calcium and magnesium concentrations in the effluent samples. **Fig. 8** shows the HCl concentration profile of the samples collected. The HCl concentration at breakthrough was measured to be 10.09 wt%.

Unlike coreflood experiments run at 0.5 cm^3/min and 2 cm^3/min, experimental runs at higher flow rates of 5, 10, 20 cm^3/min did not show face dissolution. In fact the regular acid system injected propagated through the core and produced at least one dominant wormhole with multiple branches.

Fig. 9 shows the pressure drop profile for an injection rate of 5 cm^3/min. De-ionized water was used as a preflush until the system stabilized at 200°F. The pressure drop across the core stabilized at around 170 psi before acid was injected, upon which the pressure drop increased in steps up to almost 300 psi. The wormhole terminated at the core outlet at around 300 psi pressure drop after injecting 1.81 pore volumes acid.

Absence of face dissolution at acid injection rate of at 5 cm^3/min was evident from the lower calcium concentration in the effluent samples. As HCl reacted with the carbonate rock, creating dissolution channels along the core, the calcium concentration in the effluent samples started to increase. The highest calcium and magnesium

concentration (**Fig. 10**) in the effluent samples recorded were 44,990 mg/L and 11,490 mg/L at breakthrough. Also, the acid concentration at breakthrough was reduced from 15 wt% to 11.6 wt% indicating less acid reacted with the calcite as it propagated through the core.

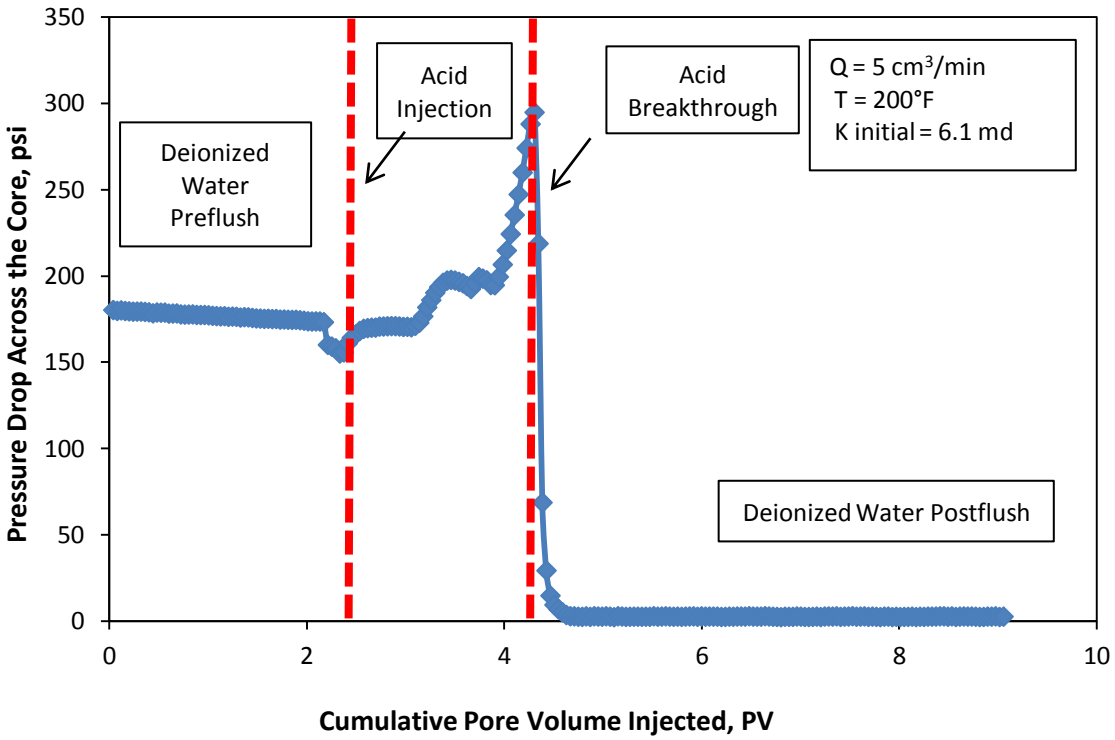

Fig. 9-Pressure drop across the water saturated core at an acid injection rate of 5 cm^3/min and 200°F.

Fig. 11 and **Fig. 12** indicate similar pressure drop across the cores at higher injection rates of 10 and 20 cm^3/min. After an initial pre-flush of de-ionized water, acid was injected. The acid system took 1.14 and 1.39 pore volume to breakthrough at 10 and 20 cm^3/min repectively. It is also evident from the calcium and magnesium profiles at

acid injection rates of 10 and 20 cm^3/min (**Fig. 13** and **Fig. 14)** that the lower flow rate took

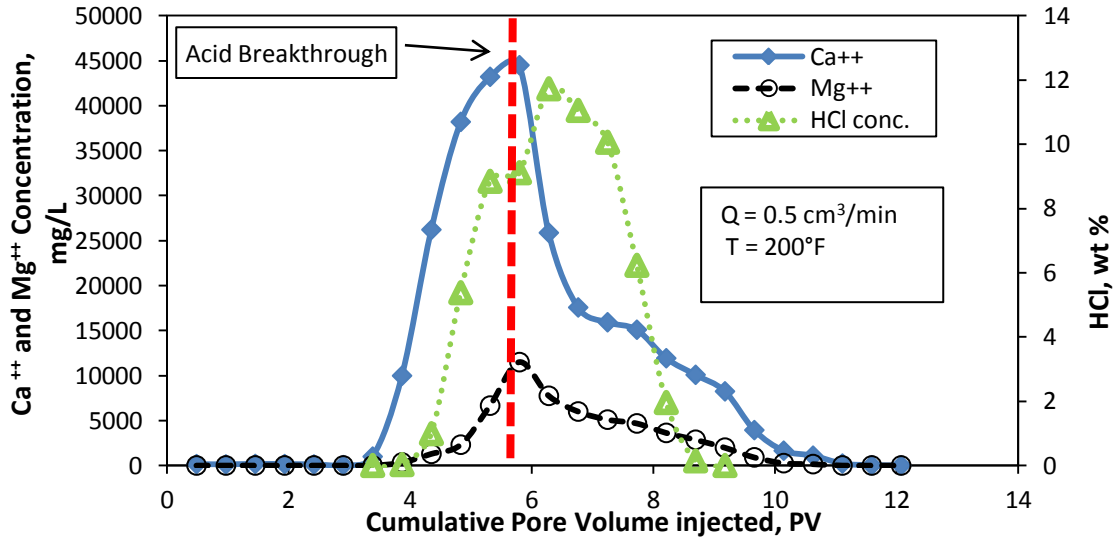

Fig. 10-Calcium, magnesium, and HCl concentrations in the effluent samples at acid injection rate of 5 cm^3/min.

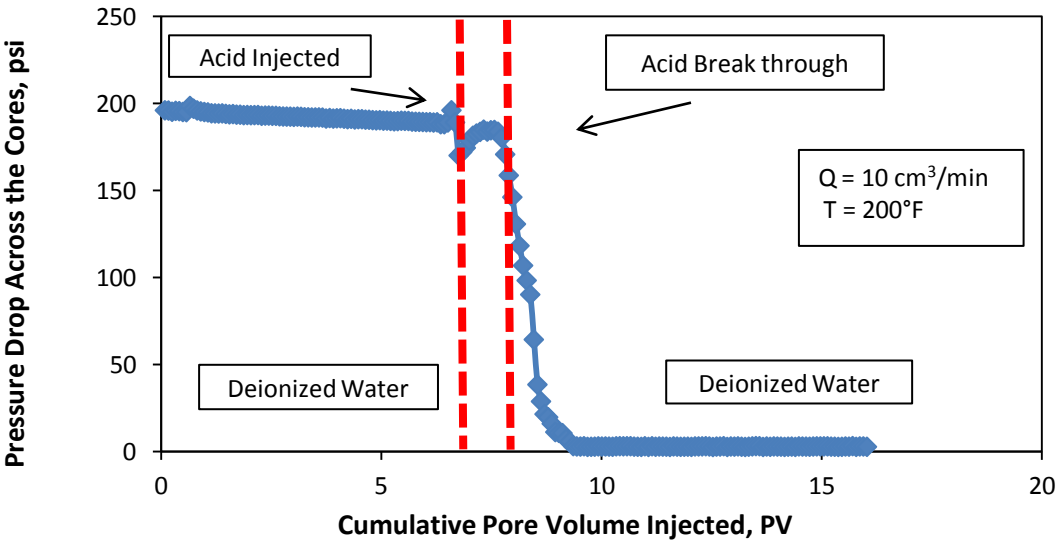

Fig. 11-Pressure drop across the water saturated core at an acid injection rate of 10 cm^3/min and 200°F.

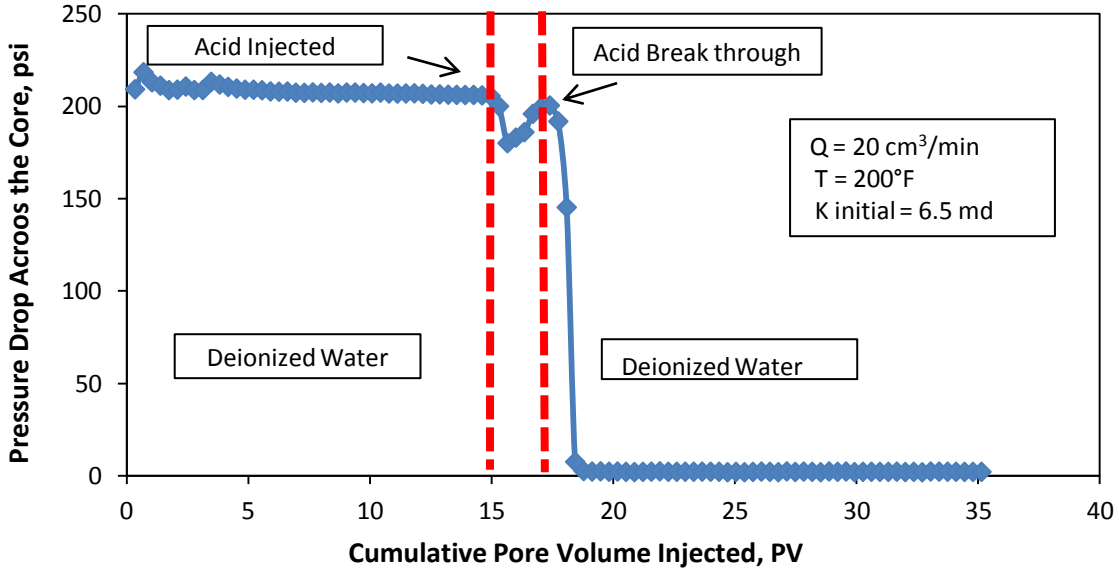

Fig. 12-Pressure drop across the water saturated core at an acid injection rate of 20 cm^3/min and 200°F.

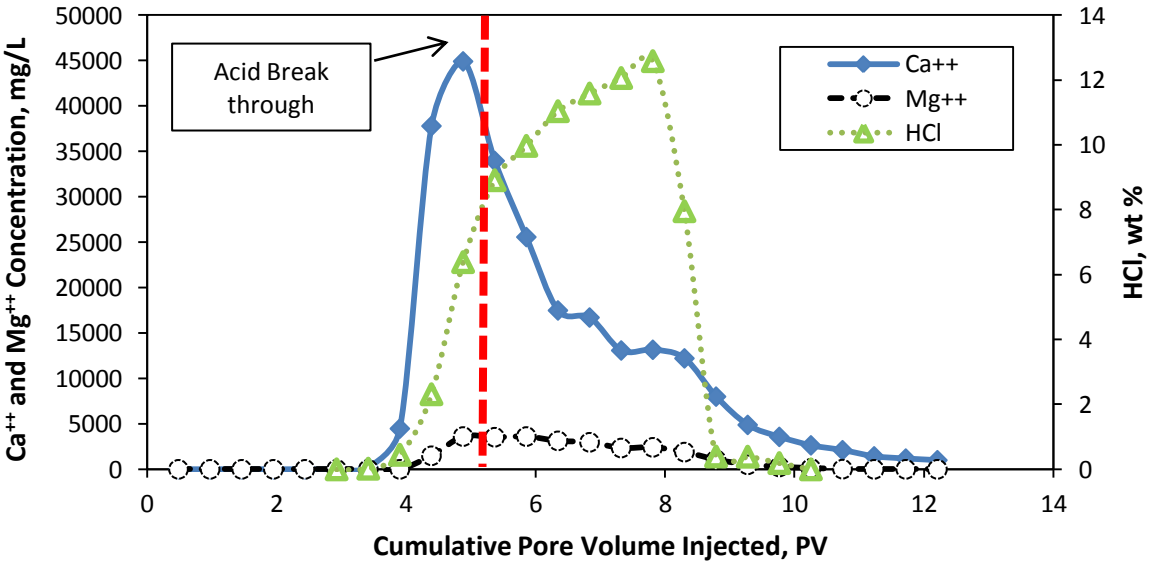

Fig. 13-Calcium, magnesium, and HCl concentrations in the effluent samples at acid injection rate of 10 cm^3/min.

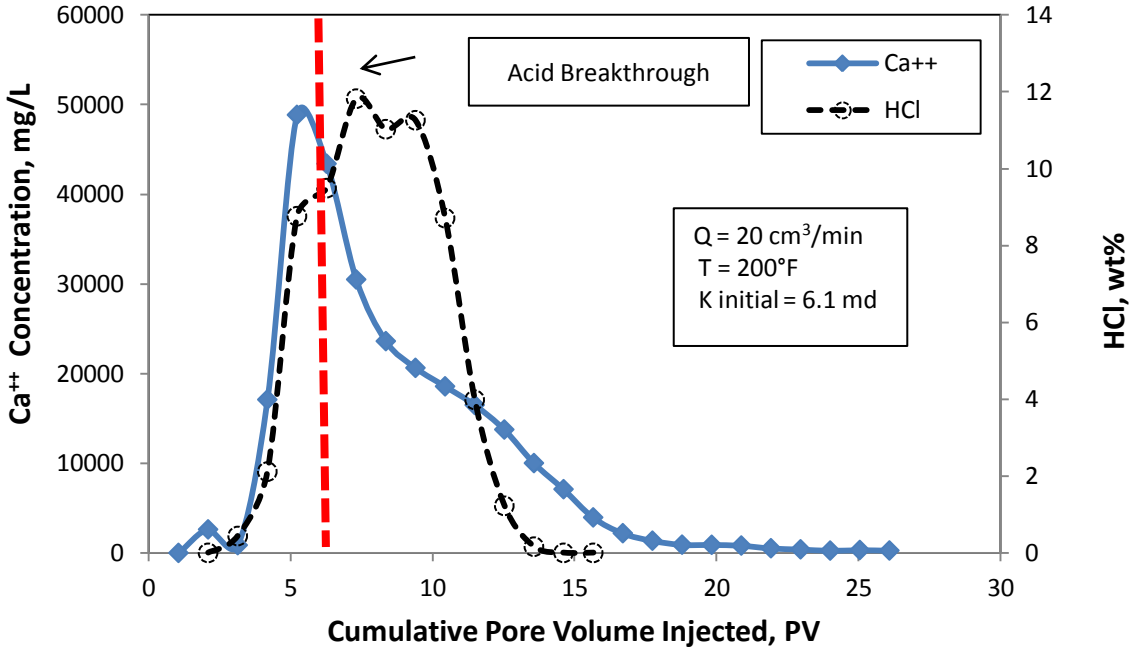

Fig. 14—Calcium, magnesium, and HCl concentrations in the effluent samples at acid injection rate of 20 cm^3/min.

fewer pore volumes to breakthrough than the higher flow rate**.** The highest calcium concentration in the effluent samples at 10 cm^3/min was measured at breakthrough to be 44,930 mg/L, while at 20 cm^3/min, the concentration rose up to 48,860 mg/L indicating greater contact time between acid and the calcite. Although effluent samples from the coreflood at 20 cm^3/min measured 3614 mg/L, it was interesting to note the absence of magnesium ions in the samples from coreflood at 10 cm^3/min. This could possibly be related to the different lithology of the core used for this coreflood at 10 cm^3/min compared to cores used for other experiments. The acid concentrations at breakthrough for both flow rates were comparable at 12.5 and 11.8 wt % for 10 and 20 cm^3/min.

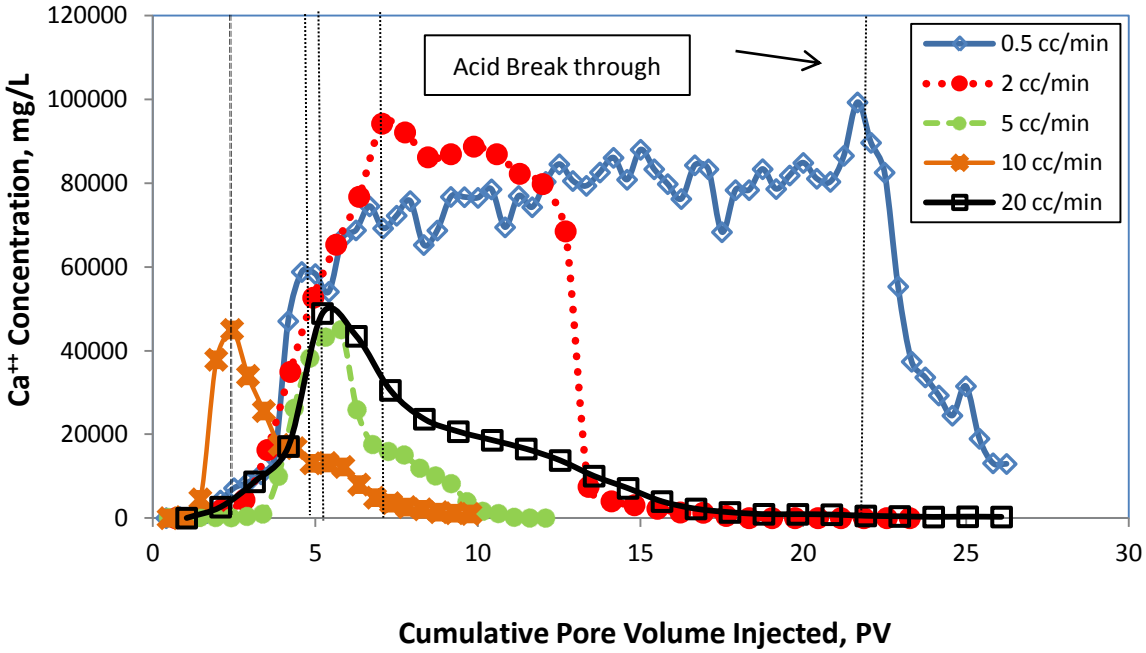

Fig. 15-Calcium concentration in the effluent samples from coreflood of water saturated cores at different injection rates.

Fig. 15 presents the ICP measured calcium concentration in the coreflood effluent samples, collected for the various experiments at different injection rates. In all cases the calcium concentration increased initially when de-ionized water preflush was switched with acid, reaching a maximum value, then decreased when the injection fluid was switched back to water. The calcium concentration is related to the amount of carbonate rock dissolved by acid, and this amount is greater for greater acid/rock contact times. Injection rates have a significant effect on the calcium concentration in the effluent samples, and hence the amount of rock dissolved during acid injection. Subsequently, the highest peak for calcium concentration was noticed at an injection rate of 0.5 cm^3/min (the least optimum case, highest contact time), while the lowest peak was

observed at an injection rate of 10 cm^3/min (the most optimum case, lowest contact time). The total calcium concentration in the effluent samples collected is represented in **Table 5.** It is clear from this table that the calcium concentration decreases as acid injection rates increase.

TABLE 5-TOTAL CALCIUM AND MAGNESIUM DISSOLVED					
Exp #	Exp. Condition	Core Diameter * Length, in.	Injection Rate, cm^3/min	Calcium dissolved, mg	Magnesium dissolved, mg
1	15 wt% HCl, 200°F	1.49 * 3.53	0.5	8874	1717
2		1.49 * 2.94	2	1965	319
3		1.48 * 3.03	5	418	89
4		1.49 * 3.32	10	733	77
5		1.49 * 2.60	20	718	0

Acid concentration for all the samples collected was compared as shown in **Fig. 16**. It is used to confirm the pore volume of acid required to breakthrough from the pressure drop analysis curve. The maximum acid concentration, which also indicates acid break through, was in the case of acid flow rate of 10 cm^3/min (12.58 wt%). This was the most optimum injection rate. The lowest acid concentration at breakthrough was measured at 0.5 cm^3/min (9.14 wt%). This was the least optimum injection rate of all the conditions tested. These results ratify the previous analysis made for calcium concentration.

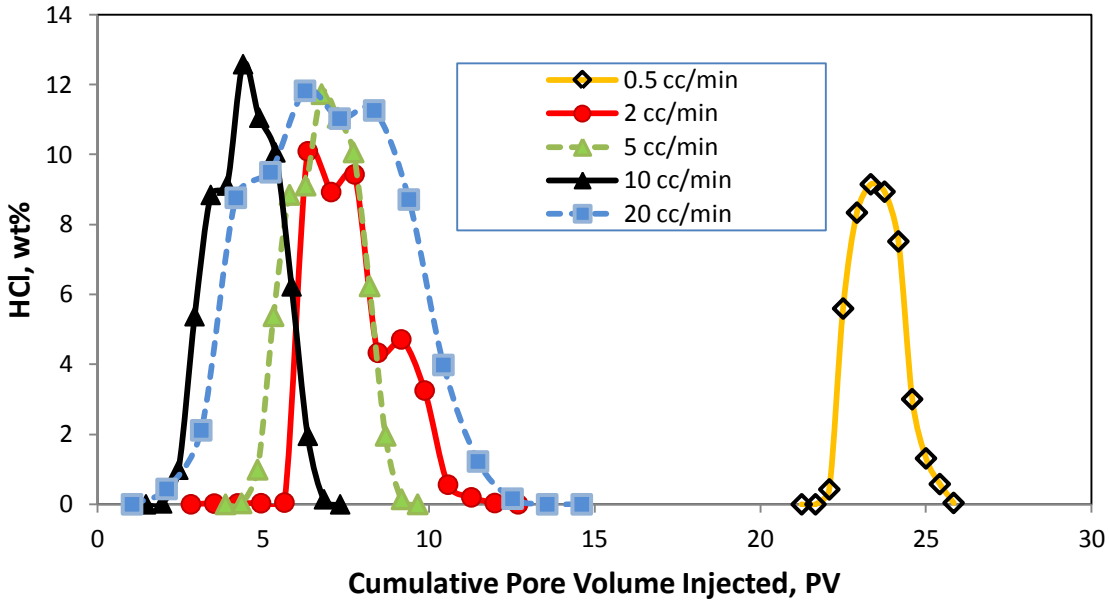

Fig. 16—HCl concentration in the effluent samples from coreflood of water saturated cores at different injection rates

Optimum Injection Rate for Water Saturated Cores

Optimum injection rate is defined as the injection rate which requires the minimum volume of acid to achieve breakthrough. Five coreflood experiments were conducted on field cores from the Middle East saturated in deionized water using regular 15 wt% HCl at 200°F. The only additive added was corrosion inhibitor. Volume of acid required to breakthrough is a function of the rock lithology and acid injection flow rate. **Fig. 17** shows the volume of acid required to breakthrough varying as a function of acid injection rate.

From this figure, it can be observed that as the injection rate increased, the volume of acid to breakthrough decreased, and reached a minimum at a rate at 10 cm^3/min.

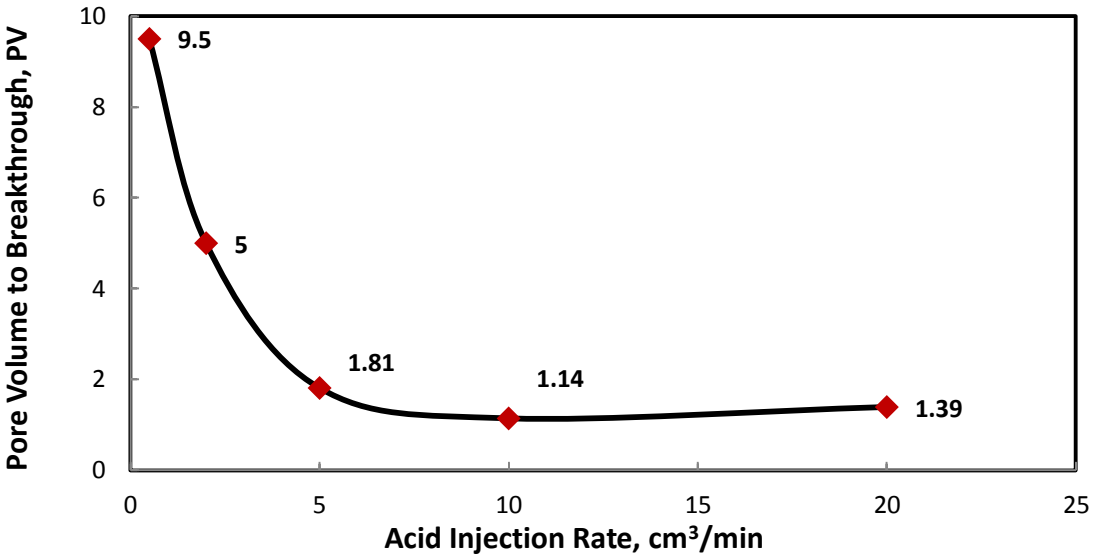

Fig. 17—Acid pore volume required to propagate wormholes through the core

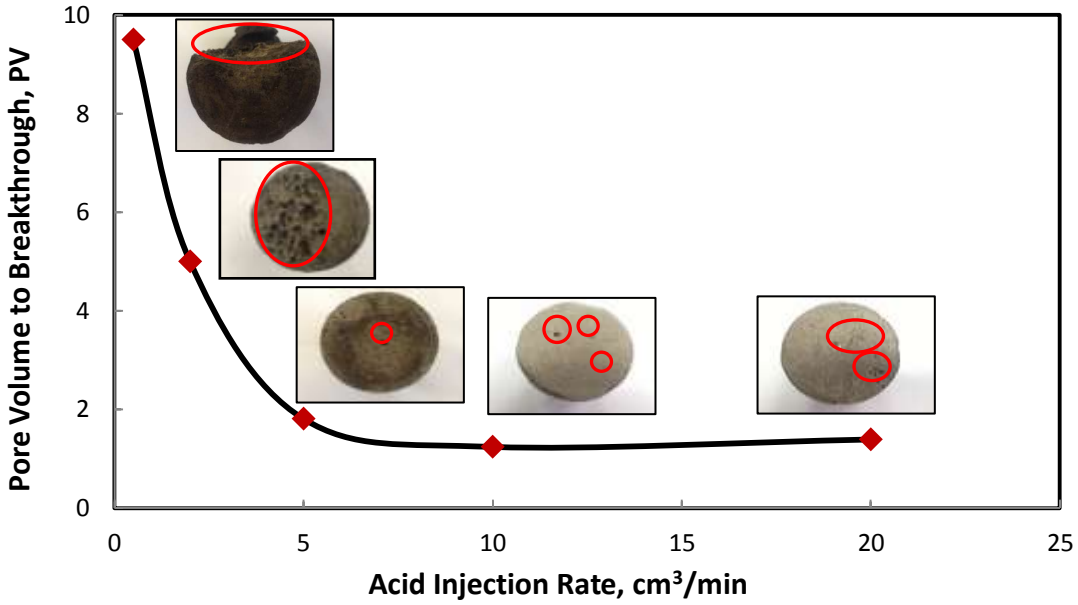

Fig. 18-Dissolution patterns identified from photographs of inlet side of core samples.

At flow rates higher than optimum injection rates, the volume of acid to achieve breakthrough increased again. However, the curve is steeper on the left side of the optimum injection rate, and relatively flat for rates higher than the optimum. This fact indicates that the effect of injection rate is more pronounced at low injection rates, where the mass transfer limited regime controls the rate of reaction. Subsequently, the surface-reaction limited regime is reached at higher injection rates, with the pore volumes to breakthrough being only slightly affected by changes in injection rate.

Photos of the inlet face of core samples taken after the acid injection has been profiled as a function of corresponding flow rate as shown in **Fig. 18**. This was done to observe the effect of the acid on the inlet face of the core, and to identify dissolution structures created by the acid reaction with the limestone rock. From **Fig. 18**, it was observed that at low injection rates (i.e. 0.5 cm^3/min), severe face dissolution washed out a portion of the core along the axial length of the sample making the acidizing process (i.e. wormhole penetration) significantly inefficient. As injection rate was increased to a flow rate of 2 cm^3/min, face dissolution and conical wormholing was observed for the core sample. When the acid injection rates were increased further to 5 and 10 cm^3/min, there was no face dissolution observed at the core inlet, and there was a tendency to create few dominant wormholes. Finally, for high injection rates (i.e. above 10 cm^3/min), several dominant wormholes are created, with increased wormhole branching as flow rate is increased. The lowest volume of acid to breakthrough was obtained when acid was injected at 10 cm^3/min, and therefore, for the conditions tested, this is considered the optimum injection rate when 15 wt% HCl was injected through limestone

cores at a temperature of 200°F. This was substantiated from the calcium and the acid concentration profile over all flow rates tested.

CT Scan Images

2D CAT scan images of the water saturated cores treated with regular acid at 200°F is shown in **Fig. 19.** Analysis of these images helps characterize the wormhole structures created at different flow rates.

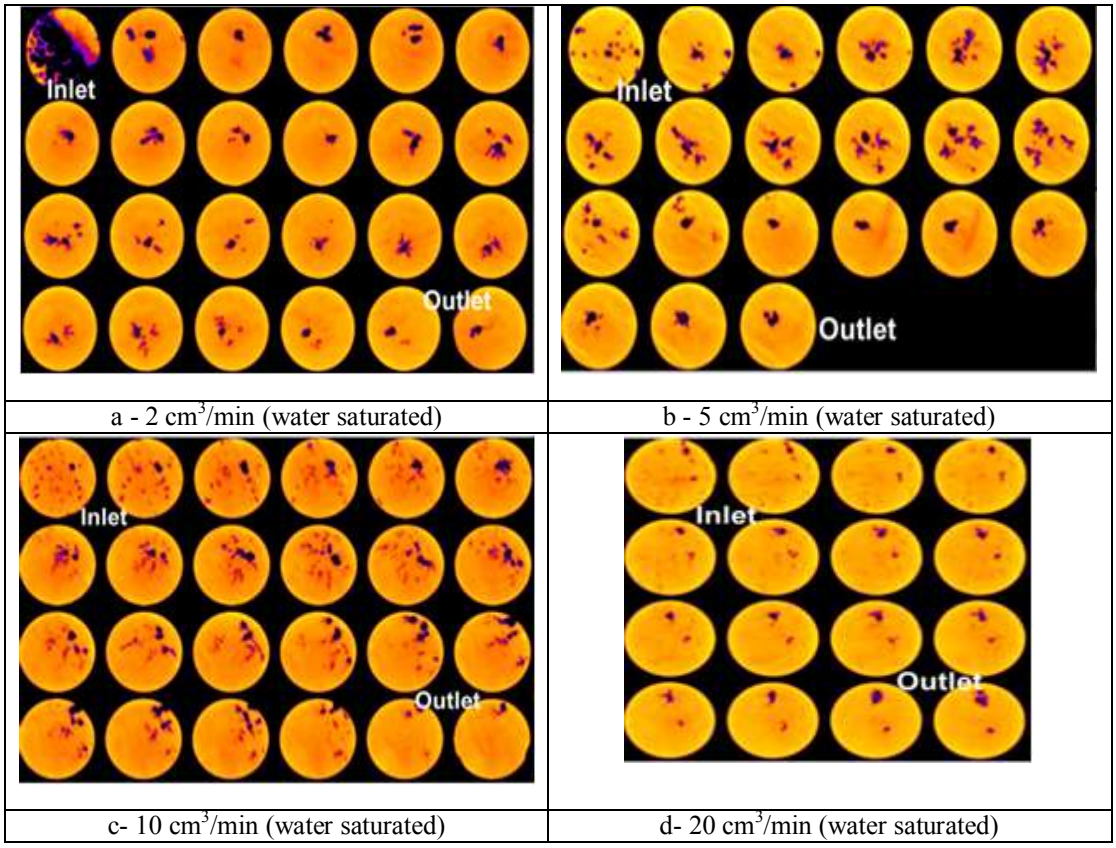

a - 2 cm^3/min (water saturated)	b - 5 cm^3/min (water saturated)
c- 10 cm^3/min (water saturated)	d- 20 cm^3/min (water saturated)

Fig. 19-CAT scan images of water saturated cores after core flood study.

Upon injection, acid starts reacting with the rock and creating wormholes. The darker spots in the image indicate low CT number and low density.

Face dissolution was noticed initially at the core inlet face for acid injection rate of $2cm^3$/min as mentioned in the previous section. The acid then propagated through the core and created a wormhole. The wormhole created at this flow rate is non optimal. HCl had achieved breakthrough at flow rates of 2 cm^3/min and above. Although the 2D images of the cores showed formation of more than more than one wormhole at the core inlet, these wormholes combined and formed a single dominant wormhole as the acid propagated towards the core outlet.

At flow rates of 10 and 20 cm^3/min, the branching of the wormhole was more dominant. This resulted in lower calcium concentration in the effluent samples compared with injection rates of 0.5 and 2 cm^3/min. At 20 cm^3/min, two dominant wormholes propagated throughout the length of the core. At 10 cm^3/min, single dominant wormhole initiated at the core inlet which increased in size and then split into two wormholes of smaller size as the acid progressed through the core. The dissolution pattern created at this injection rate resulted in the most efficient stimulation of the core.

CHAPTER IV

COREFLOOD STUDY ON WATERFLOOD RESIDUAL OIL CORES

Waterflood residual oil cores were acidized using the hydrochloric acid system using the coreflood setup shown in **Fig. 2**. **Table 1** summarizes all the data from the coreflood study of cores with residual oil. Coreflood runs were performed using 15 wt% HCl at injection rates of 0.5, 1, 5, 10, 20 cm^3/min.

Coreflood Study

Pressure drop across the core during the injection of regular acid at an injection rate of 0.5cm^3/min and 200°F is shown in **Fig. 20**. Acid injection initiated after a stable pressure drop was achieved during the preflush of 5 wt% KCl brine. Due to the high permeability of the core used (77 md), the maximum pressure drop achieved by the core during the acid injection was around 7.8 psi. 1.1 pore volumes of acid were injected before it broke through and the pressure drop stabilized at around 2.7 psi. A post flush of 5 wt% brine followed this process. Pressure drop across the core during injection of regular acid at 0.5 cm^3/min and 200°F is shown in **Fig. 20.** Unlike pressure drop curves seen during acidization of brine saturated cores at low injection rates, the cycling trend of the pressure drop curve that follows the injection of acid was not observed here. It was interesting to note the absence of face washout after acid injection. The calcium and

acid concentration in effluent samples at 0.5 cm^3/min are represented as functions of cumulative pore volume of fluid injected in **Fig. 21**. The calcium concentration in the

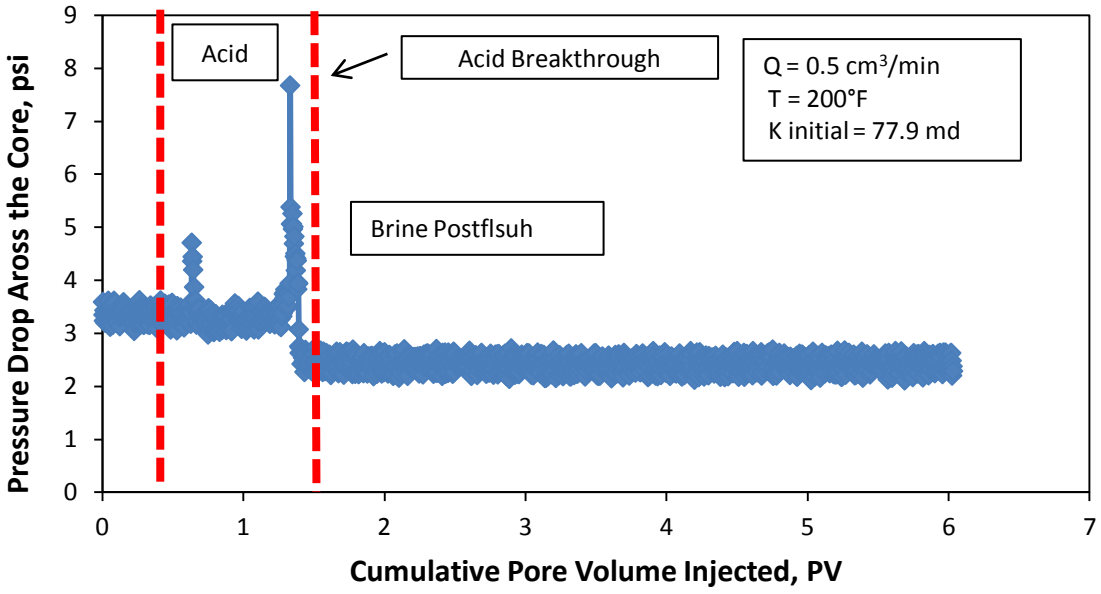

Fig. 20—Pressure drop across waterflood residual oil cores at an acid injection rate of 0.5 cm^3/min and 200°F.

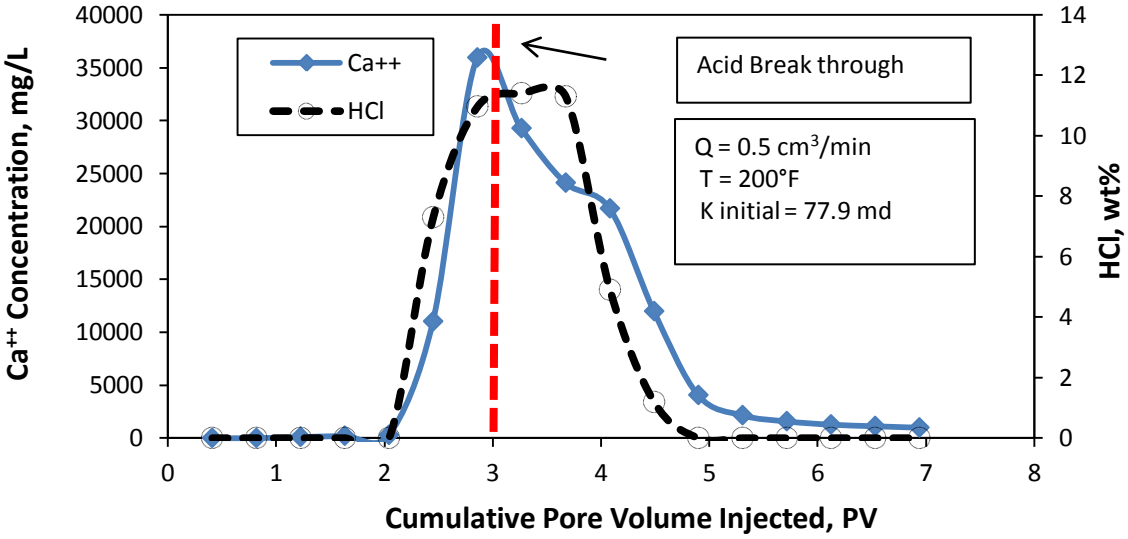

Fig. 21—Calcium and HCl concentration in the effluent samples from coreflood of waterflood residual oil cores at acid injection rate of 0.5 cm^3/min.

samples measured 35,950 mg/L at acid breakthrough. The lower concentration of calcium ions in the effluent samples in comparison with samples from the same flow rate for water saturated cores results from the absence of face dissolution in waterflood residual oil cores. Also, the acid concentration fell from an initial concentration of 15 wt% to 11.4 wt%. at breakthrough indicating low acid reactivity with the calcite rock.

The pressure drop across the core at a flow rate of 1 cm^3/min dropped from 23 psi to around 2-3 psi upon acid injection consuming just 0.83 pore volumes of acid to breakthrough as seen in **Fig. 22.** The low pore volume to breakthrough indicated that the acid was efficient in creating a dominant wormhole with minimal branches.

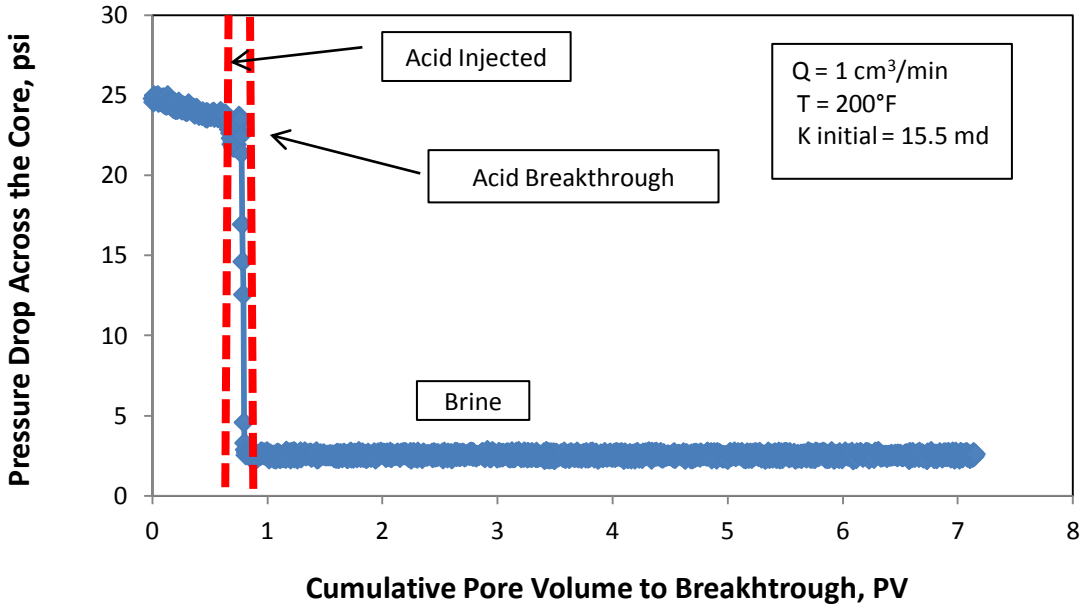

Fig. 22—Pressure drop across waterflood residual oil cores at an acid injection rate of 1 cm^3/min and 200°F.

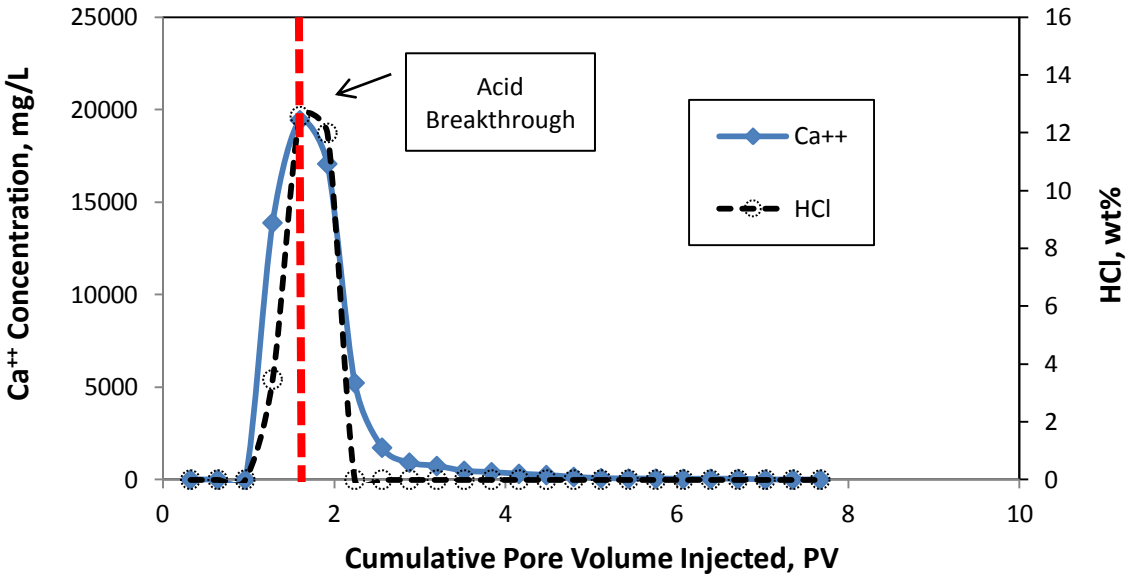

Fig. 23—Calcium and HCl concentration in the effluent samples from coreflood of waterflood residual oil cores at acid injection rate of 1 cm^3/min.

Effluent samples collected at acid injection of 1 cm^3/min resulted in a measured calcium concentration of 19,430 mg/L at breakthrough **(Fig. 23)**. This was lower than the corresponding calcium concentration collected during acid injection of 0.5 cm^3/min. Also, the acid concentration at breakthrough reduced from 15 wt% to 12.5 wt% (**Fig. 23**) indicating that the residence time and consequently the reactivity of acid with calcite rock is lesser as flow rate increases. In order to confirm the same, coreflood experiments were conducted at higher flow rates of 5, 10, 20 cm^3/min. The pressure drop across the cores during acid injection at these flow rates behave similar to each other (**Figs. 24 and 25)**. After achieving a stable pressure drop during brine preflush, acid was injected. The pressure drop across the cores dropped within 1-2 pore volumes pore volumes of acid

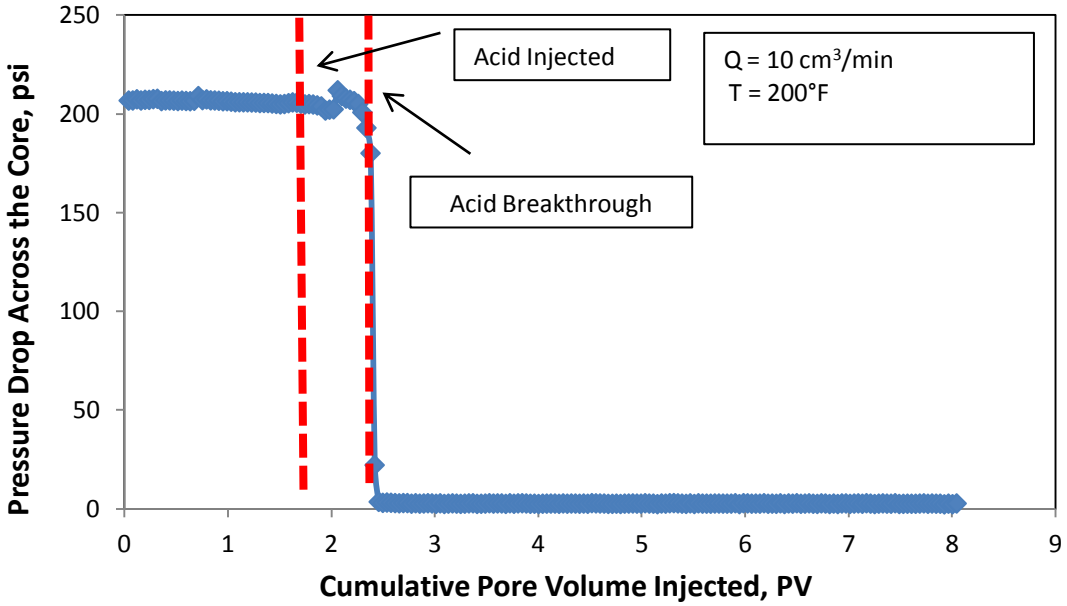

Fig. 24—Pressure drop across waterflood residual oil cores at an acid injection rate of 10 cm^3/min and 200°F.

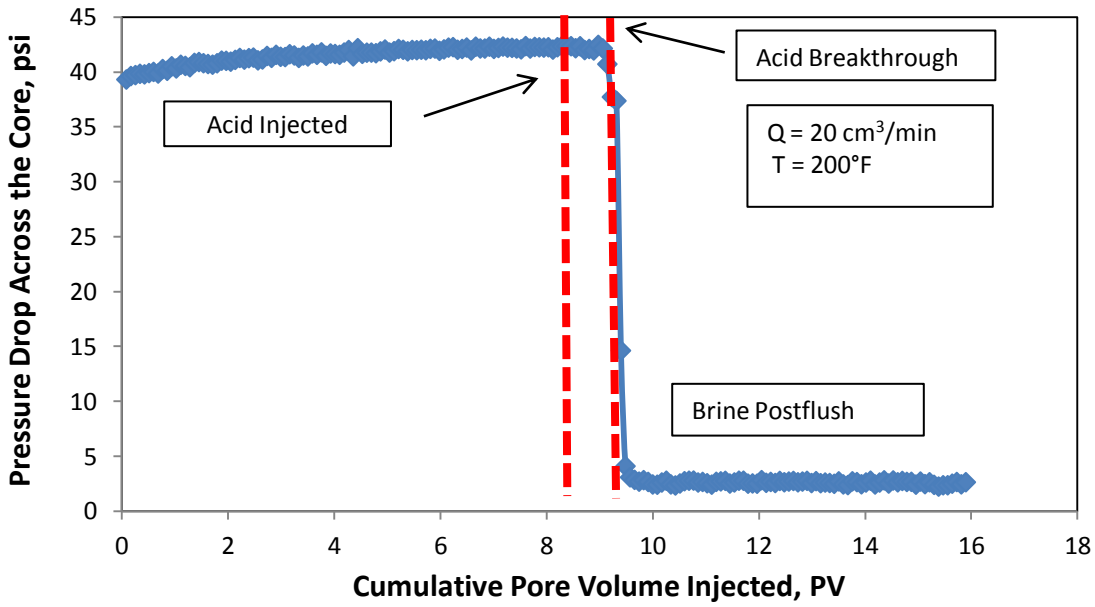

Fig. 25—Pressure drop across waterflood residual oil cores at an acid injection rate of 20 cm^3/min and 200°F.

injected indicating wormhole breakthrough. While the acid required similar pore volumes to breakthrough for 5 and 10 cm^3/min (0.68 and 0.67 respectively), the pore volume for breakthrough at 20 cm^3/min was calculated close to 0.61. The overall trend in pore volume to breakthrough indicated a decrease in acid pore volumes to breakthrough from 1.1 at 0.5 cm^3/min to 0.61 at 20 cm^3/min.

Figs. 26-28 show the calcium and acid concentration profile for acid injections at 5, 10, 20 cm^3/min as a function of cumulative fluid injected. Maximum calcium concentrations in these samples ranged from 20,720 mg/L to 32,450 mg/L at acid breakthrough. Unlike water saturated cores, the maximum acid concentration in the effluent samples from all the experiments run on waterflood residual oil cores did not reduce significantly from the initial acid concentration of 15 wt%. This is an indicator that the presence of residual oil did have an effect on the acidizing process.

Fig. 29 shows the calcium concentration profile for all the experiments run on waterflood residual oil cores. Comparison of **Fig. 15** with **Fig. 29** shows that the amount of calcium dissolved in effluent fluid samples in the case of cores saturated with water was higher than calcium measured in effluent samples from cores that contained residual oil. This further confirms our argument that oil has an effect on the acidizing process because the oil present in residual saturation forms a film on the rock grain structure and retards the acid reaction with the rock. For the same reason, at higher-injection rates acid formed finer emulsions with oil. These finer emulsions sheared and divided into smaller droplets, and produced better retardation and longer penetration. Also, at higher

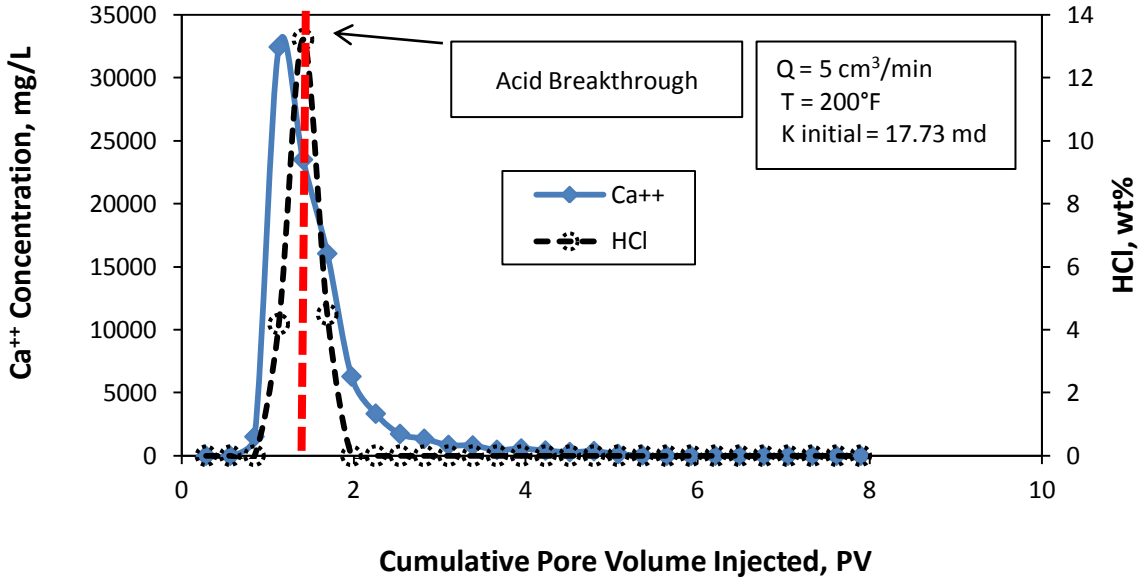

Fig. 26—Calcium and HCl concentration in the effluent samples from coreflood of waterflood residual oil cores at acid injection rate of 5 cm^3/min.

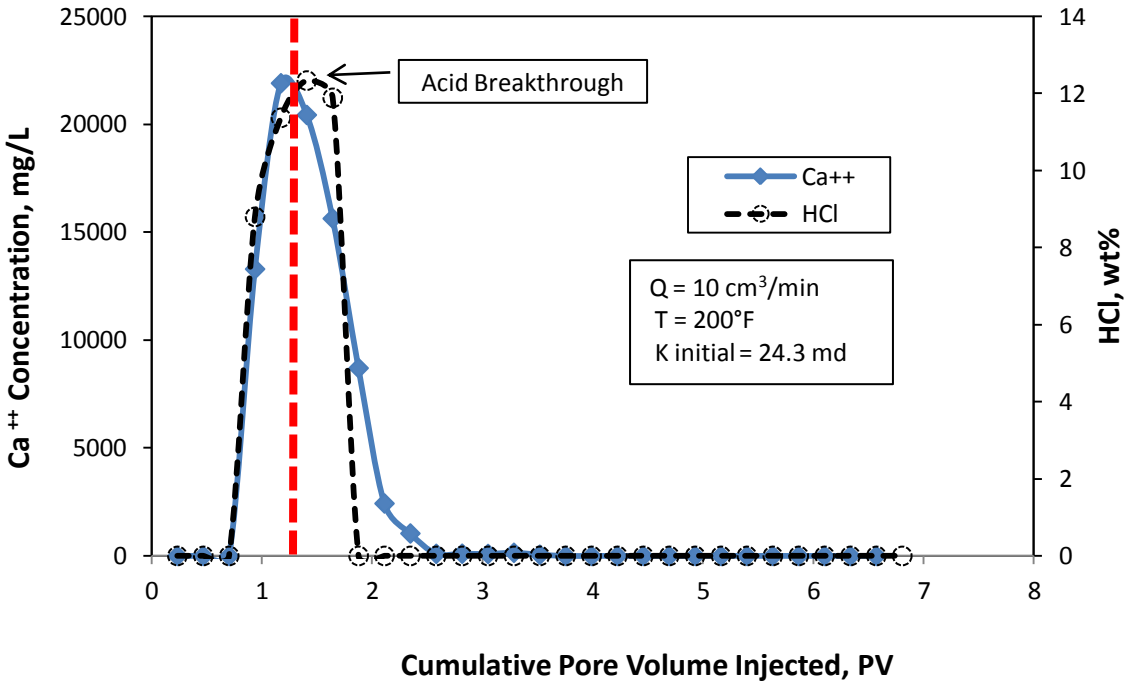

Fig. 27—Calcium and HCl concentration in the effluent samples from coreflood of waterflood residual oil cores at acid injection rate of 10 cm^3/min.

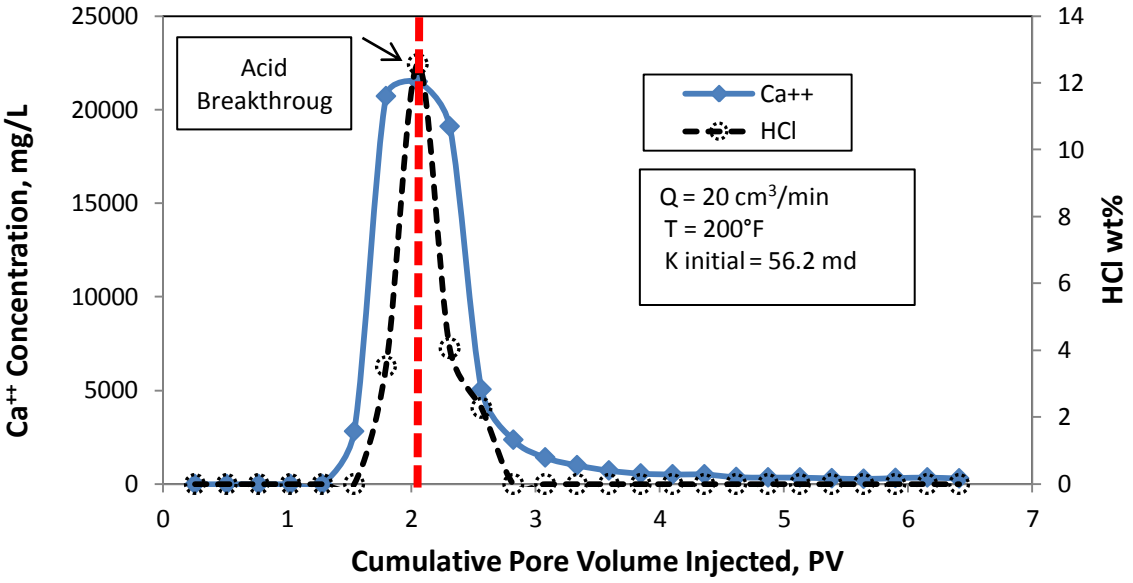

Fig. 28—Calcium and HCl concentration in the effluent samples from coreflood of waterflood residual oil cores at acid injection rate of 20 cm^3/min.

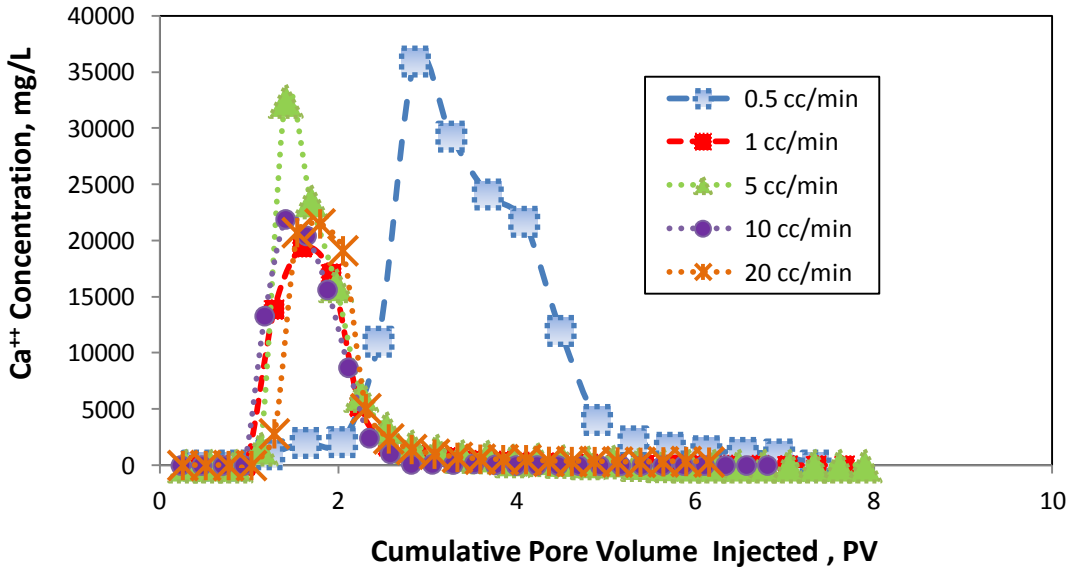

Fig. 29—Calcium concentration in the effluent samples from coreflood of waterflood residual oil cores at different injection rates.

injection rates acid is forced to flow through paths generated by brine. This results in less branching out of the wormhole.

CT Scan Images of Waterflood Residual Oil Cores – Post Coreflood

2D CAT scan images of the cores with residual oil treated with regular acid at 200°F are shown in **Fig. 30.** Unlike acid injection at low flow rates through water saturated cores, no face dissolution was noticed at the core inlet face for any of the injection rates studied. Regular acid was able to achieve breakthrough at all flow rates. The significant difference in calcium concentration in effluent samples observed for all the injection rates can be explained with the aid of the CT scan images of the cores after the experiment.

At 1cm^3/min, a single dominant wormhole with minimal branching propagated through the core length. At acid injection of 5 cm^3/min the wormhole split into three smaller channels as the acid made its way through the core, and at 10 cm^3/min the wormhole formed was not as pronounced as the ones formed at lower flow rates. At 20 cm^3/min, regular acid created wormholes with branches which acted as ideal high spots for more acid to react with the rock. This resulted in acid dissolving more sample matrix, and thus higher concentration of calcium ions in the effluent sample were observed. It is imperative to consider the factor that the cores used were only 3 in. and even after switching to brine after breakthrough, the acid present in the flow lines contribute in shaping the wormhole. Thus, CT images cannot be used as the sole criteria to decide on the optimum injection rate.

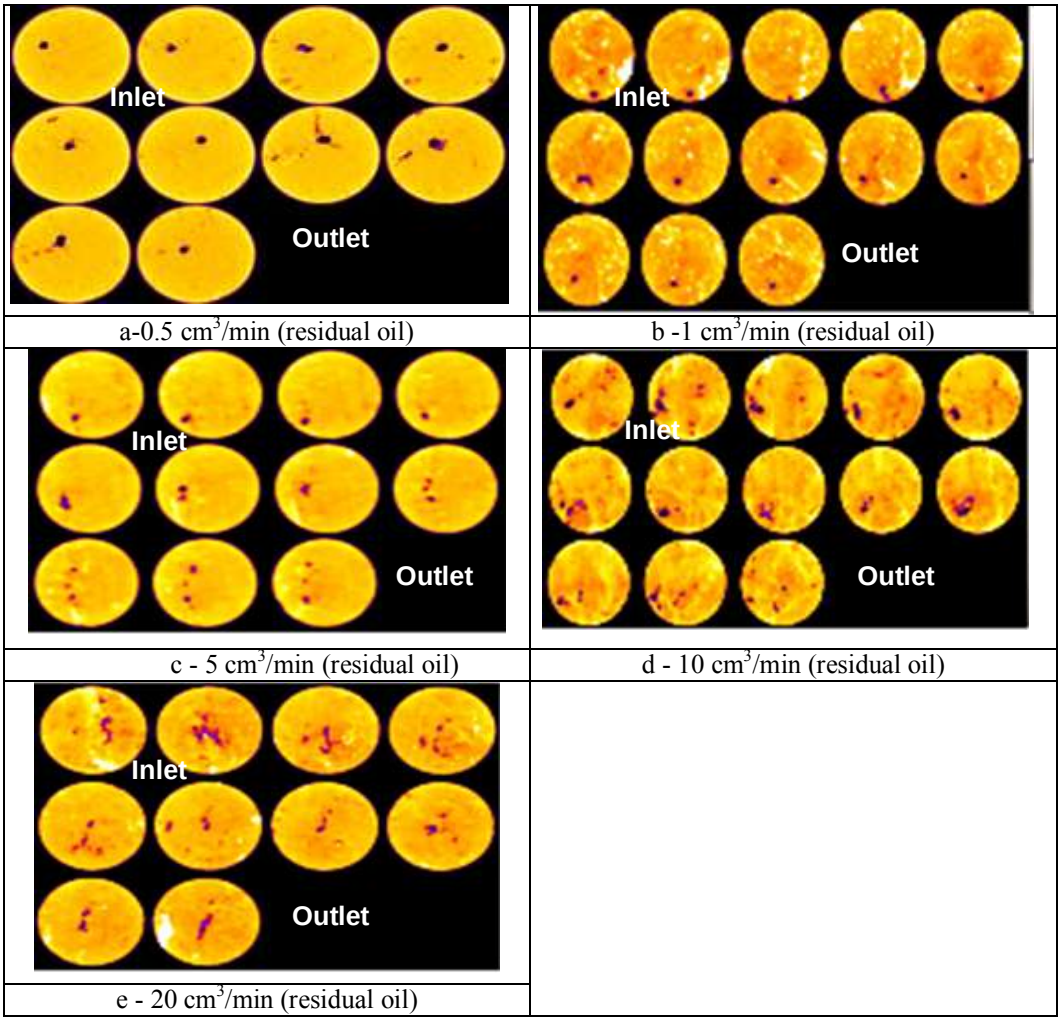

a-0.5 cm^3/min (residual oil)

b -1 cm^3/min (residual oil)

c - 5 cm^3/min (residual oil)

d - 10 cm^3/min (residual oil)

e - 20 cm^3/min (residual oil)

Fig. 30—CAT scan images of waterflood residual oil cores after core flood study.

Optimum Injection Rate for Waterflood Residual Oil Cores

Five coreflood experiments were also conducted on cores with residual crude oil using regular 15 wt% acid at 200°F. KCl-brine preflush and post flush was used. In case of cores with residual oil, the actual pore volume of the core is not available for flow because a portion of the core volume is occupied by residual oil which cannot be

removed. Here, the definition of acid pore volume to breakthrough is slightly different from the previous case where the entire pore volume was saturated with water. In cores with residual oil, pore volume to breakthrough was calculated as the volume of acid required to propagate a wormhole through the core considering only the effective pore space available for flow.

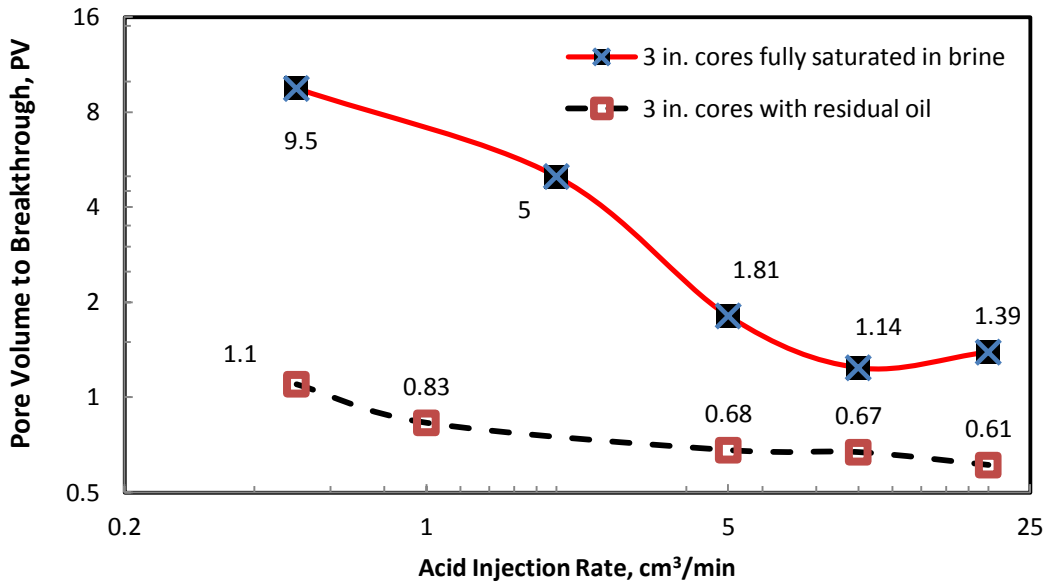

Fig. 31—Comparison of acid pore volume to breakthrough through the water saturated cores and waterflood residual oil cores (Logarithmic scale).

Fig. 31 shows the relationship between pore volumes of acid to break through for water saturated cores and waterflood residual oil cores against acid injection rate. From **Fig. 31,** as the injection rate increases, the volume of acid required for breakthrough decreases. The increased efficiency of acid in propagating wormholes at higher flow rates is caused of shearing of the acid-oil emulsion, which causes longer penetrations

with minimal branching. Another possible explanation of this phenomenon is that residual oil could have formed a screen between acid and rock, preventing acid from reacting with calcite, and forcing it to flow through channels created by the brine. Thus, acid injections on cores with residual oil require less pore volume to breakthrough compared to cores saturated with deionized water. Also, no optimum acid injection rate was observed for the core floods run on waterflood residual oil cores.

CHAPTER V

COREFLOOD STUDY ON OIL SATURATED CORES

Table 1 summarizes all the data from the coreflood study of cores saturated in naphthenic crude oil. Indiana Limestone cores saturated in oil were loaded into the core holder and an overburden and back pressure were applied. Coreflood runs were performed using 15 wt% HCl at injection rates of 1, 5, 10, and 20 cm^3/min. All the core flood experiments were performed at 200°F. No preflush was used prior to acid injection. After the system achieved at temperature of 200°F, acid was injected. The flooding test was terminated when a constant pressure drop was determined. 5 wt% KCl-Brine was injected as a post flush.

Coreflood on Oil Saturated Cores

Pressure drop across the core during the injection of regular acid at an injection rate of 1 cm^3/min and 200°F is shown in **Fig. 32.** Since no pre-flush was used, an initial rise in pressure drop was noticed the instant acid was injected. After injection of 3 pore volumes of acid, the pressure drop rose sharply to around 47 psi from 17 psi followed by acid breakthrough. The rise in pressure drop is because of the acid reaching the core inlet and consequent reaction. The pressure drop increased until the acid pushed the oil in the flow channels and found a region of least resistance and highest permeability and changed its direction of flow within the core. This behavior continued as the acid propagated through the core and the wormhole broke through at the core outlet.

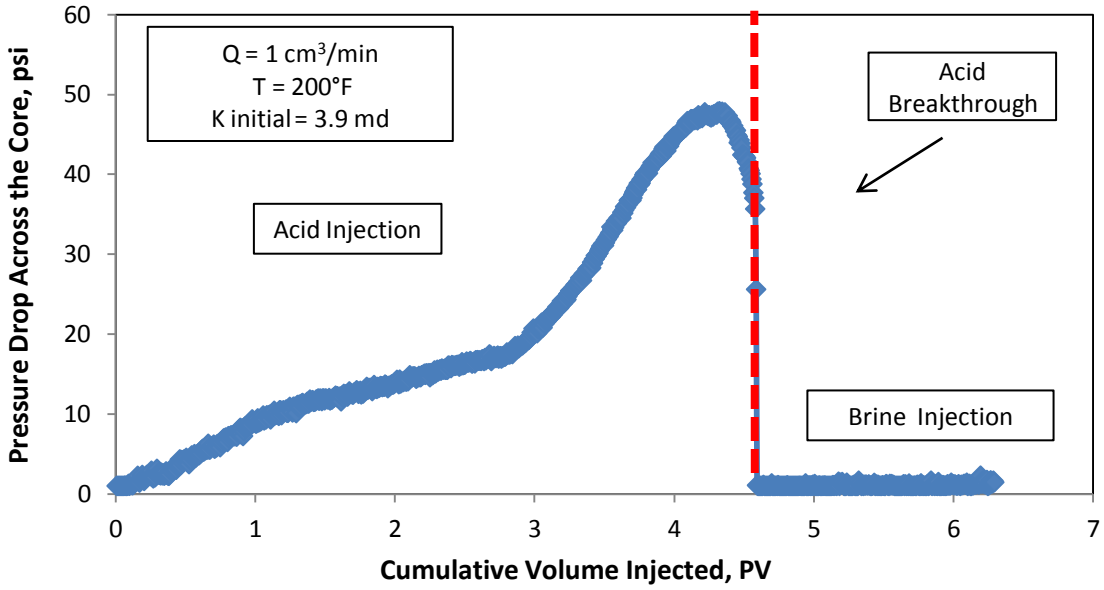

Fig. 32—Pressure drop across oil saturated core at an acid injection rate of 1 cm^3/min and 200°F.

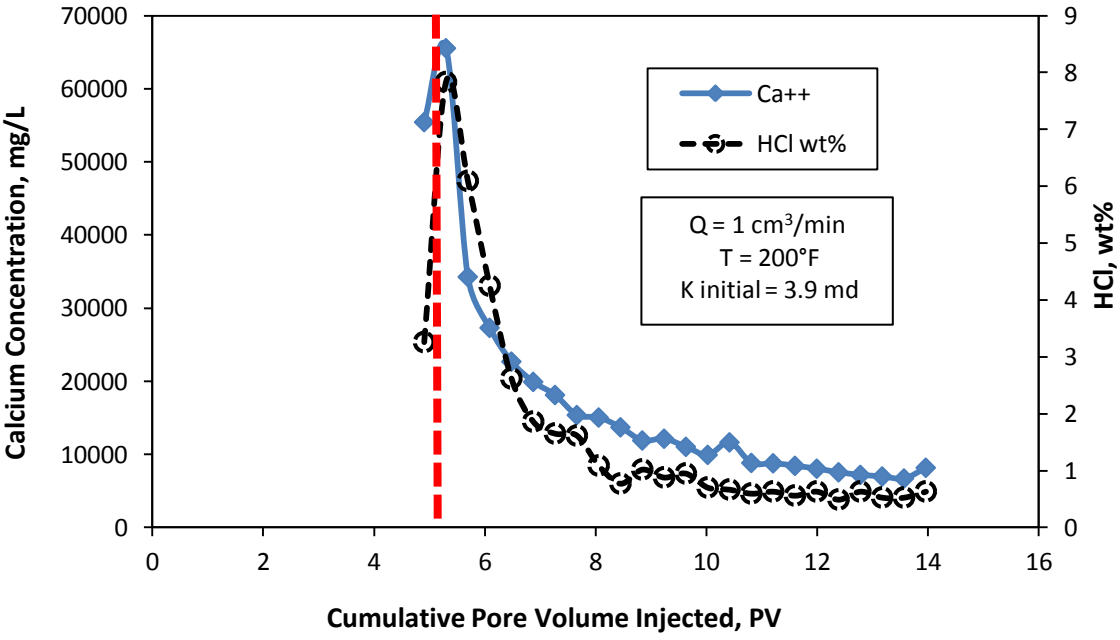

Fig. 33-Calcium and HCl concentration in the effluent samples from coreflood of oil saturated cores at acid injection rate of 1 cm^3/min.

Unlike water saturated cores, the cycling trend of the pressure drop that follows the injection of acid at low injection rates was not observed. This could either mean that the back pressure applied kept the CO_2 formed from the dissolution of rock in solution or that there was not a sufficient reaction between the acid and rock to start with.

Fig. 34—Acid face dissolution of oil saturated cores at 0.5 cm^3/min and 200°F.

.

However, there was some face dissolution observed at the core inlet which accounted for as much as 4.51 pore volumes of acid required for acid breakthrough. The pressure dropped after injection of 4.51 pore volumes of acid to around 2 psi indicating acid breakthrough. Upon acid breakthrough, acid injection was stopped and 5 wt% KCl was injected. Also, **Fig. 34** indicates formation of multiple wormholes at the core outlet, suggesting that injection of acid at this rate was not the most ideal for stimulation of the core.

The acid concentration in effluent samples at 1 cm^3/min was profiled as shown in **Fig. 33**. The highest effluent acid concentration of 7.8 wt% marks the point of acid

breakthrough. Once the wormhole was formed and acid broke through, the partially reacted acid made its way through the core and reached the core outlet.

The highest calcium concentration of 65,530 mg/L was recorded at breakthrough. This was comparatively lower than the corresponding calcium concentration observed for water saturated and residual oil cores. The oil present in the flow channels not only provided resistance to the flow of acid but also retarded its reactivity due to the presence of oil around the pore grain.

At an injection rate of 5 cm^3/min the pressure drop peaked at 138 psi upon acid injection, and then dipped sharply as HCl broke through the core. 3.9 pore volumes of acid was required for break through. Pressure drop across the core during injection of regular acid at 5 cm^3/min and 200°F is shown in **Fig. 35**.

It was interesting to note that the degree of face dissolution observed at 5 cm^3/min was not as prominent as the one observed at 1 cm^3/min (**Fig. 37**). This also justifies the fact that the acid took less pore volume to breakthrough at 5 cm^3/min as compared to 1 cm^3/min. The calcium and HCl concentration in the effluent samples for an acid injection rate of 5 cm^3/min has been profiled using **Fig. 36**. The calcium concentration at breakthrough was measured to be 71,430 mg/L.

Fig. 38 and Fig. 39 indicate similar pressure drop patterns across the cores at higher injection rates of 10 and 20 cm^3/min. Although the cores used had similar initial permeability, the pressure drop peak for 20 cm^3/min was higher than that at 10 cm^3/min

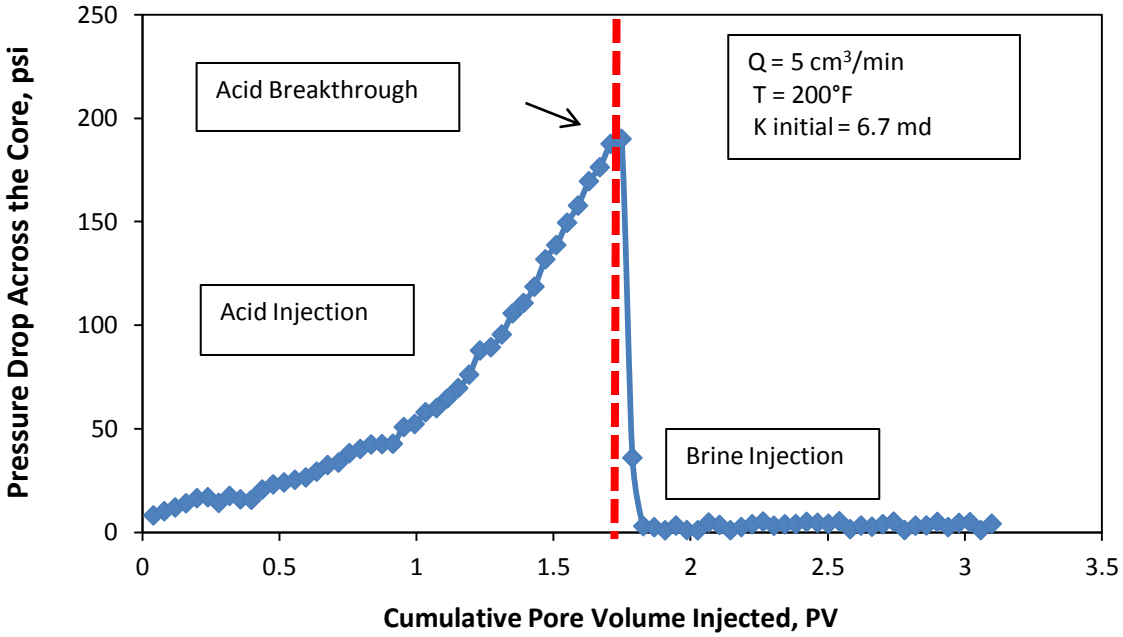

Fig. 35—Pressure drop across oil saturated core at an acid injection rate of 5 cm^3/min and 200°F.

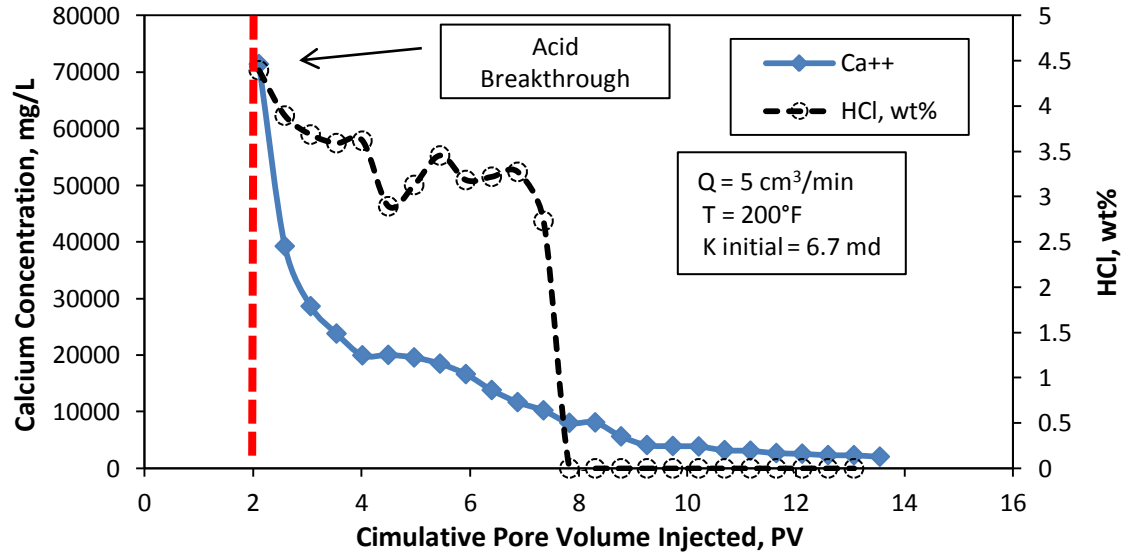

Fig. 36—Calcium and HCl concentration in the effluent samples from coreflood of oil saturated cores at acid injection rate of 5 cm^3/min.

Fig. 37—Inlet and outlet face oil saturated cores at 5 cm^3/min and 200°F.

because of a greater resistance from oil saturating the core at higher flow rates. The acid system took 5.12 and 3.91 pore volumes to breakthrough at 10 and 20 cm^3/min respectively.

Fig. 40 and Fig. 41 represent the calcium concentration profile for acid injection rates of 10 and 20 cm^3/min respectively. Calcium concentration for 10 cm^3/min peaked at breakthrough with a value close to 82,660 mg/L while the maximum calcium concentration recorded at acid injection of 20 cm^3/min was only 36,530 mg/L. This justifies why the former took greater pore volumes to breakthrough. Also, the inlet face of the core after acid injection at 10 cm^3/min (**Fig. 42-a)** suggests formation of multiple wormholes. **Fig. 42-b** shows the inlet and outlet face of core at 20 cm^3/min. Acid concentration in the effluent samples from core flood at 10 and 20 cm^3/min (**Fig. 40 and Fig. 41)** shows that more acid was spent in creating a wormhole in the former case than the latter.

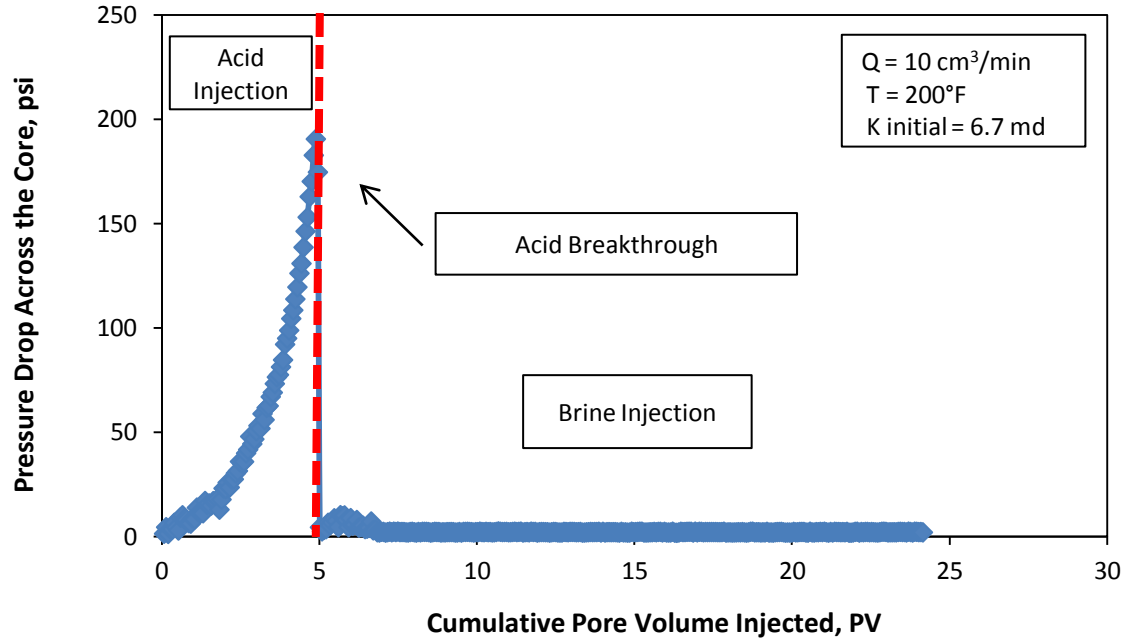

Fig. 38-Pressure drop across oil saturated core at an acid injection rate of 10 cm^3/min and 200°F.

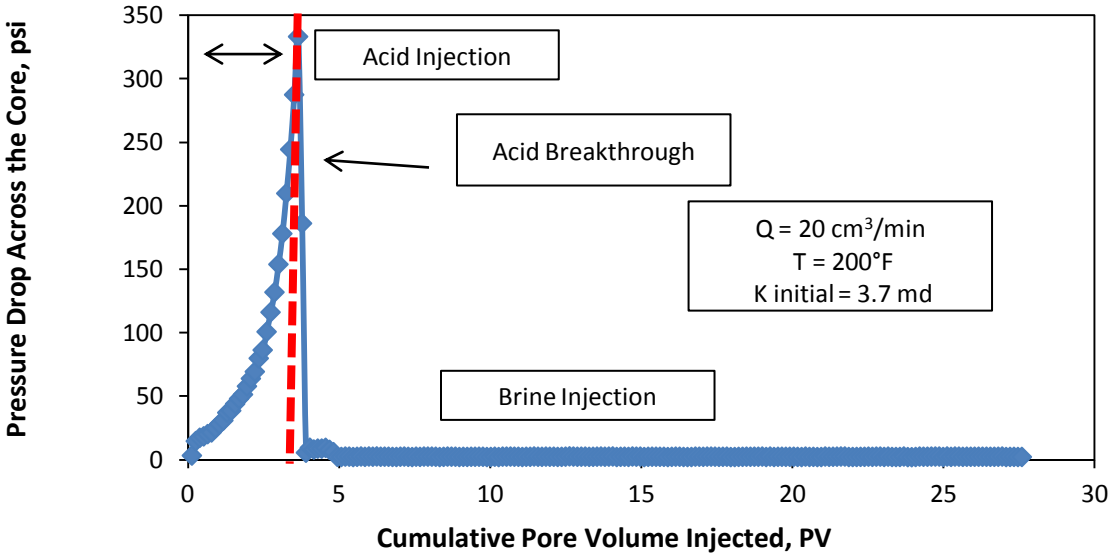

Fig. 39-Pressure drop across oil saturated core at an acid injection rate of 20 cm^3/min and 200°F.

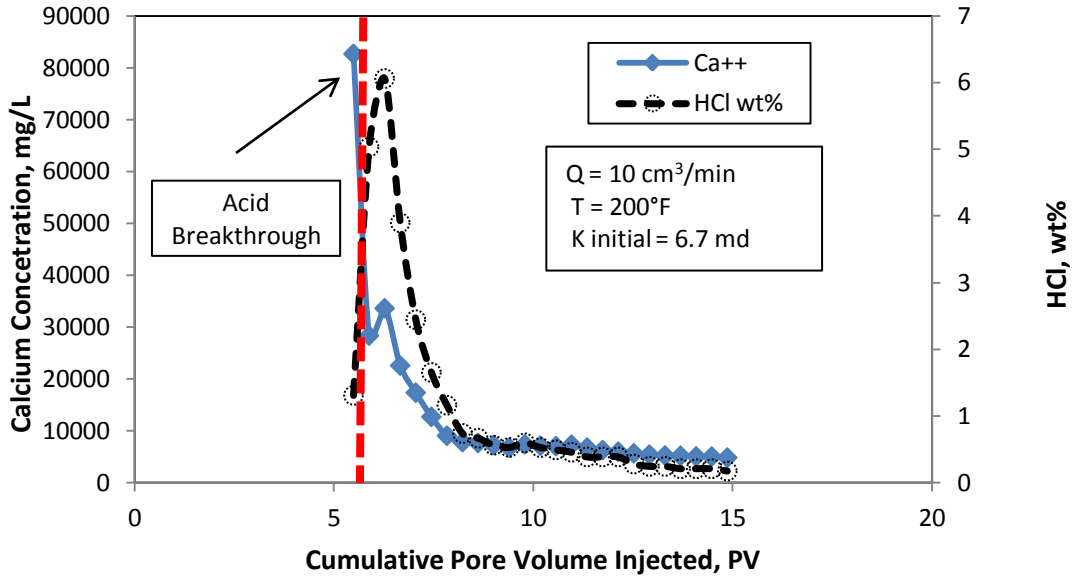

Fig. 40-Calcium and HCl concentration in the effluent samples from coreflood of oil saturated cores at acid injection rate of 10 cm^3/min.

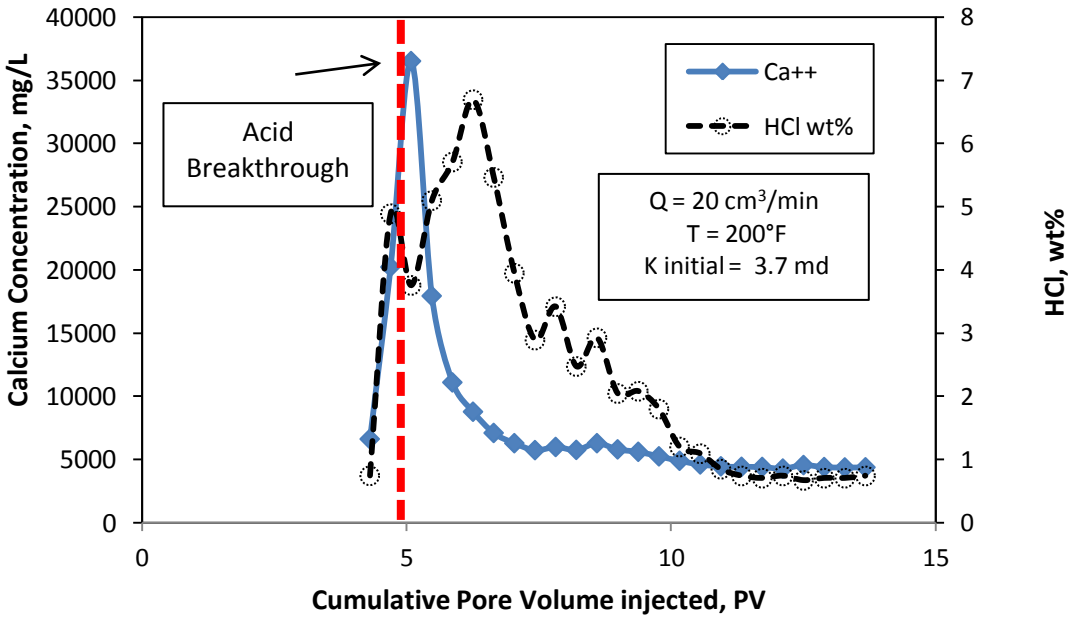

Fig. 41-Calcium and HCl concentration in the effluent samples from coreflood of oil saturated cores at acid injection rate of 20 cm^3/min.

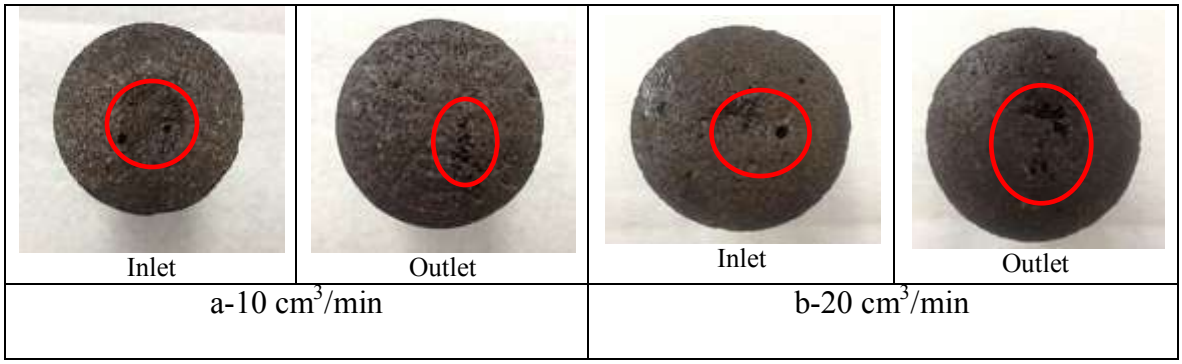

Fig. 42—Inlet and outlet face oil saturated cores at 10 and 20 cm^3/min and 200°F.

Fig. 43 shows the calcium concentration profile for all the experiments run on oil saturated cores. Comparison of **Fig. 43** with **Fig. 15** and **Fig. 29** show that the amount of calcium dissolved in effluent fluid samples in the case of waterflood residual oil cores was the least of the three cases tested. This further confirms our argument that residual oil has an effect on the acidizing process.

Optimum Injection Rate for Oil Saturated Cores

Four coreflood experiments were also conducted on cores saturated in crude oil using regular 15 wt% acid at 200°F. KCl-brine post flush was used. There was no clear relationship observed between pore volumes to breakthrough and the acid injection rate.

In fact, the pore volume to breakthrough showed a declining trend with increasing flow rate up to 5 cm^3/min after which acid took greater pore volumes to breakthrough. However, there a decline in PV_{bt} at higher injection rate of 20 cm^3/min after peaking at 10 cm^3/min.

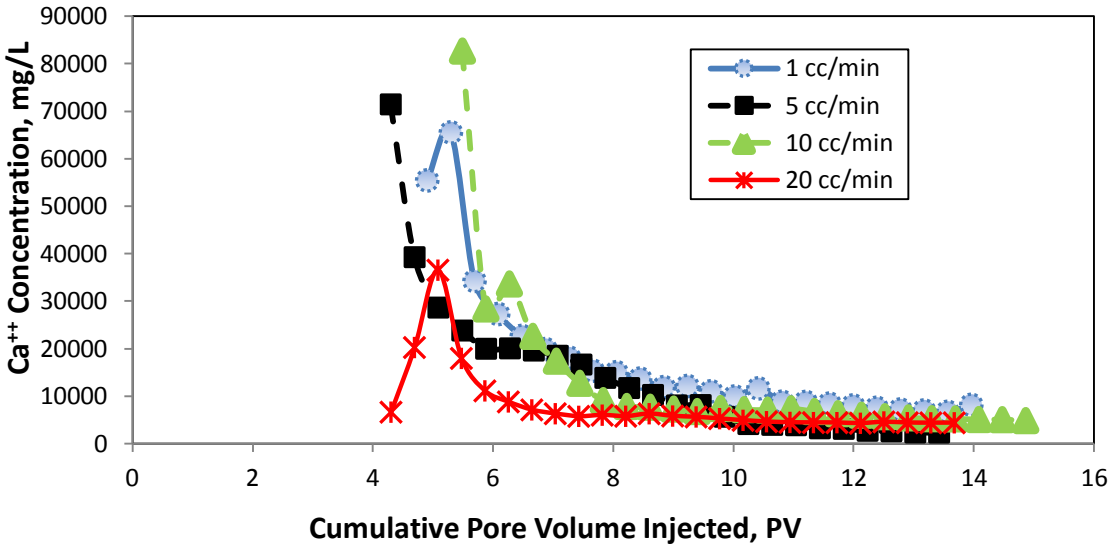

Fig. 43—Calcium concentration in the effluent samples from coreflood of oil saturated cores at different injection rates.

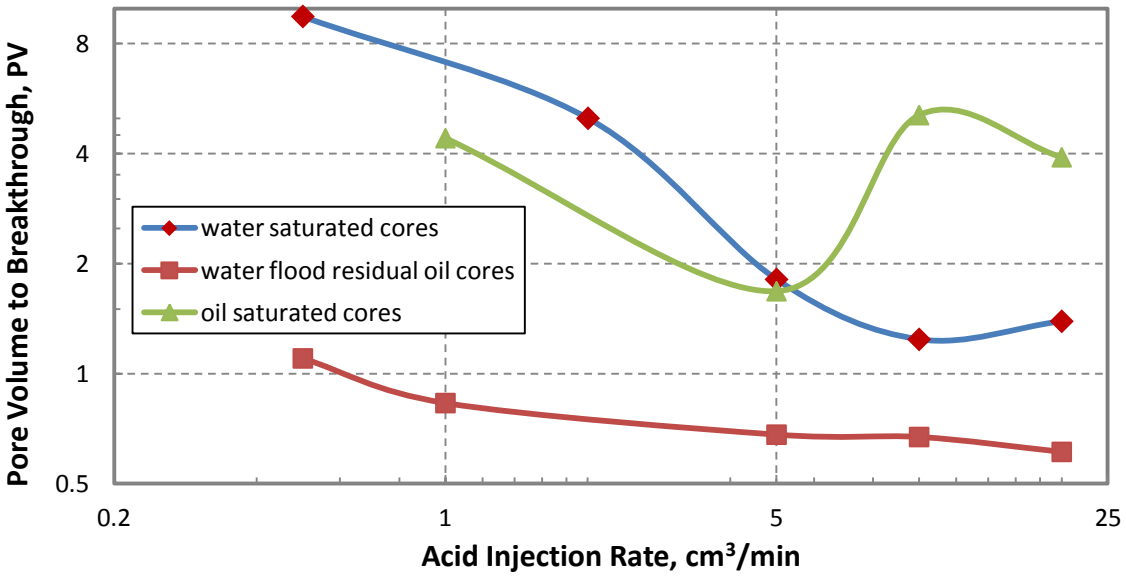

Fig. 44—Comparison of acid pore volume to breakthrough through the water saturated cores, oil saturated cores and waterflood residual oil cores.

Fig. 44 shows the relationship between pore volumes of acid to break through for water saturated, oil saturated, and waterflood residual oil cores against acid injection rate. Oil saturated cores took the highest acid pore volumes to breakthrough among the three saturation conditions except at low injection rates where severe face washout accounted for greater volumes of acid being consumed during wormhole propagation through brine saturated cores. High pore volumes to breakthrough for oil saturated cores could be attributed to a cumulative effect of the retardation of acid reactivity with the rock and the resistance to the flow of acid by oil whose viscosity is 3 times that of the acid being injected. Thus, the decrease in PV_{bt} for oil saturated cores at high acid injection rates could be a result of viscous fingering of acid through the crude oil.

CHAPTER VI

COMPARATIVE COREFLOOD STUDY ON CORES UNDER VARIOUS SATURATION CONDITIONS

Three coreflood experiments were performed using a regular acid system to confirm the absence of face dissolution or washout of the core face at low injection rate on Indiana Limestone cores. The cores used were of dimensions 6 in. length and 1.5 in. diameter. The first coreflood was conducted on brine saturated core, second on a core fully saturated in oil and the third coreflood on waterflood residual oil core. All the experiments were performed at an acid injection rate of 0.5 cm^3/min and at 200°F.

Brine Saturated Cores

The pressure drop curve for the 6 in. brine saturated core behaved similarly to the curve for the 3 in. core at same flow rate. From **Fig. 45,** the pressure drop across the core stabilized at 23.8 psi during water injection, followed by an initial rise in pressure drop, the instant acid was injected. This is because of the sudden rise in viscosity of the fluids flowing through the lines when 5 wt% KCl brine was switched with acid. The cycling trend of the pressure drop curve was observed because of CO_2 release similar to the 3 in. core following acid injection at 0.5 cm^3/min. A large portion of the core was dissolved in acid, which released CO_2 from solution. 4.4 pore volumes of acid were injected until the pressure drop fell from 43.5 psi to of 2.11 psi. The sudden drop in pressure indicated

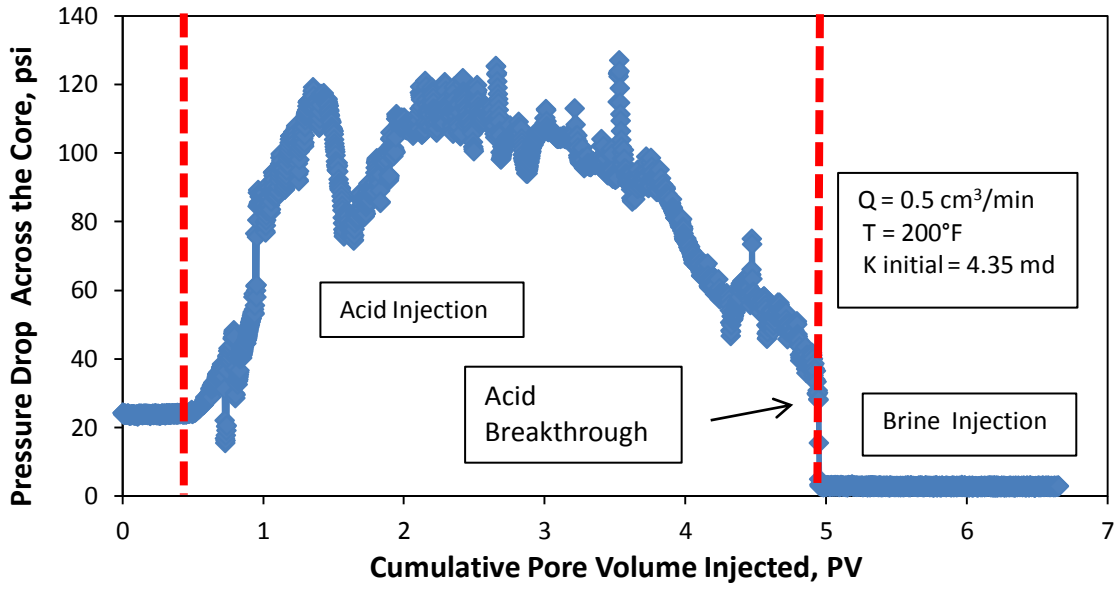

Fig. 45—Pressure drop across brine saturated 6 in. core at an acid injection rate of 0.5 cm^3/min and 200°F.

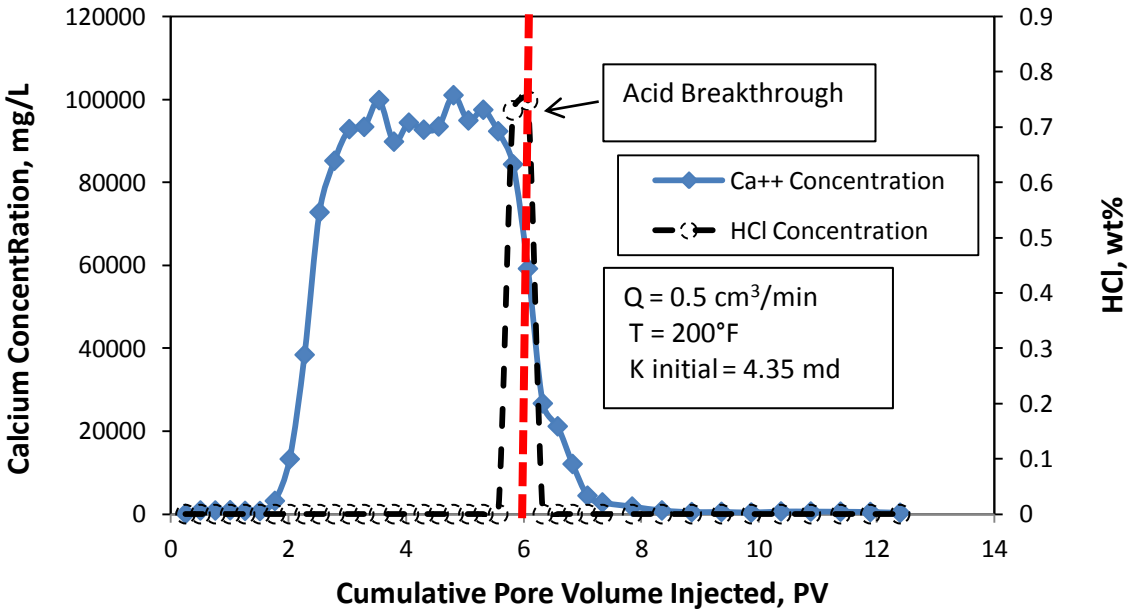

Fig. 46—Calcium and HCl concentration in the effluent samples from coreflood of brine saturated 6 in. core at acid injection rate of 0.5 cm^3/min.

Fig. 47—Inlet and outlet face of brine saturated 6 in. core at 0.5 cm^3/min and 200°F.

acid breakthrough. Upon acid breakthrough acid injection was stopped and brine was injected as a post flush.

Fig. 47 shows washout across the cross section of the core because of high leakoff rate which accounted for higher pore volume to break through. Although the pore volume to break through across this core was found to be as high as 4.5, the acid took lesser pore volume to breakthrough compared to cores of 3 in. in length., wherein almost 9.5 pore volumes of acid was consumed. This indicated that the length of the core does have an effect on the pore volume to breakthrough.

Fig. 46 shows the calcium and HCl profiles for the same experiment. The highest calcium concentration in the effluent samples (101,000 mg/L) measured higher than that from coreflood experiment of 3 in. cores in spite of taking lesser pore volume to breakthrough. This could be accounted for by the fact that the acid left in the lines after breakthrough continued to dissolve the core even after switching from acid to brine. The low acid concentration of 0.7 wt% found in the effluent samples at breakthrough justifies this explanation.

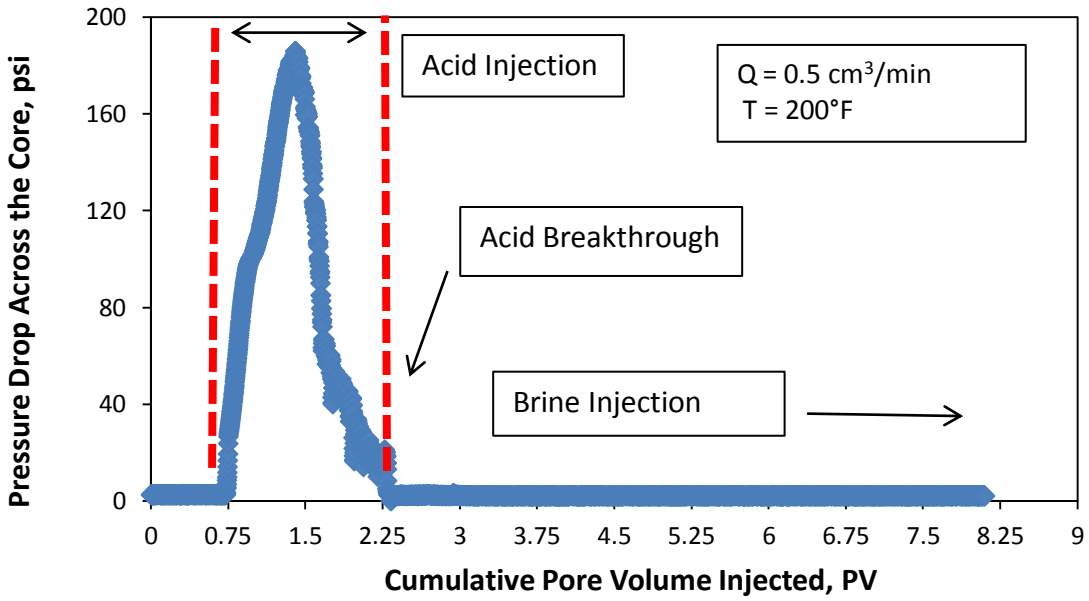

Fig. 48—Pressure drop across oil saturated 6 in. core at an acid injection rate of 0.5 cm^3/min and 200°F.

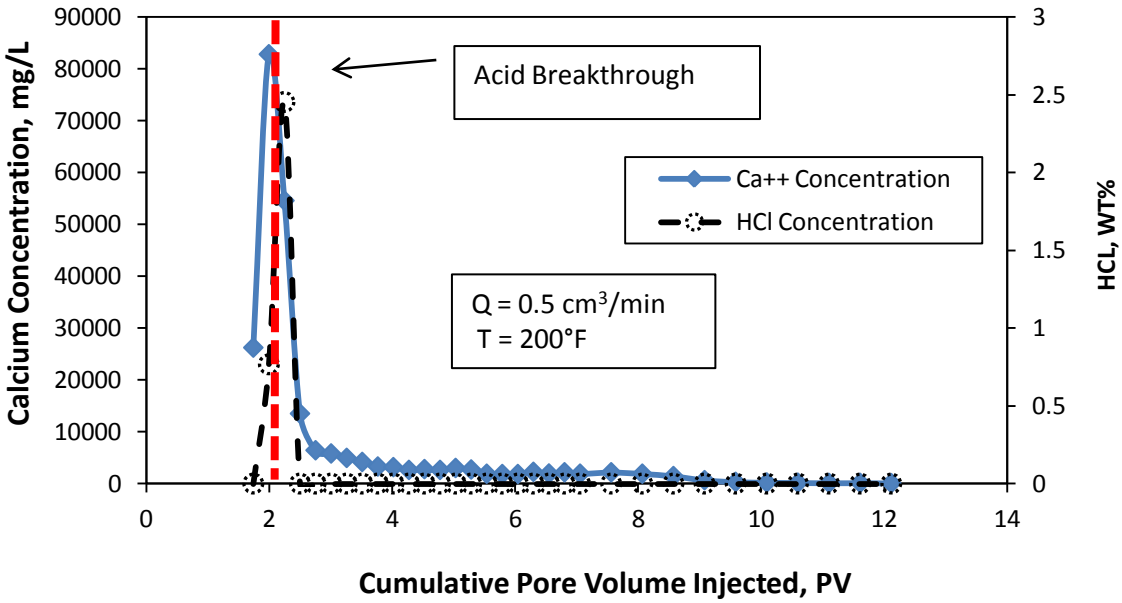

Fig. 49—Calcium and HCl concentration in the effluent samples from coreflood of oil saturated 6 in. core at acid injection rate of 0.5 cm^3/min.

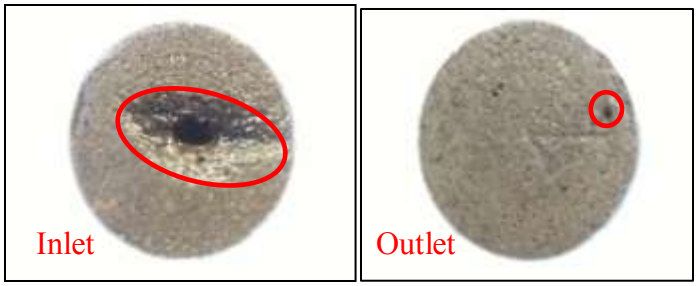

Fig. 50—Inlet and outlet face of oil saturated 6 in. core at 0.5 cm^3/min and 200°F.

Fully Saturated in Oil

Upon injection of acid through the core fully saturated in oil, the pressure drop across the core peaked at 185.3 psi, followed by a gradual drop in pressure drop indicating wormhole formation in progress **(Fig. 48)**. Once the pressure drop was reduced to 2-3 psi, it was confirmed that 1.43 pore volumes of acid were required for breakthrough break through to occur.

The inlet and outlet face of the core shown in **Fig. 50** suggests formation of a conical wormhole. The calcium profile plotted in **Fig. 49** indicates that the relative concentration of calcium ions in the effluent samples from coreflood experiments conducted on oil saturated cores were less than the concentration recorded for brine saturated cores. This is because the degree of dissolution at the core inlet was less for oil saturated cores. Also, the acid concentration at breakthrough was 2.5 wt % (**Fig. 49**), which is higher than the corresponding concentration for brine saturated cores.

Cores with Waterflood Residual Oil

Fig. 51 shows the pressure drop curve for the core flood on the waterflood residual oil core. A 5 wt% KCl was used as a preflush before injecting acid. Upon injection of acid, the pressure drop increased to 130.8 psi, followed by a drop in pressure at breakthrough after injection of 0.68 pore volumes of acid. 5 wt% KCl brine was used. Calcium and acid concentrations at recorded at breakthrough were close to 66,180 mg/L and 4.07 respectively **(Fig. 52)**. It was interesting to note that there was no face dissolution observed, which confirmed our findings from experiments conducted on 3 in. cores (**Fig. 53**).

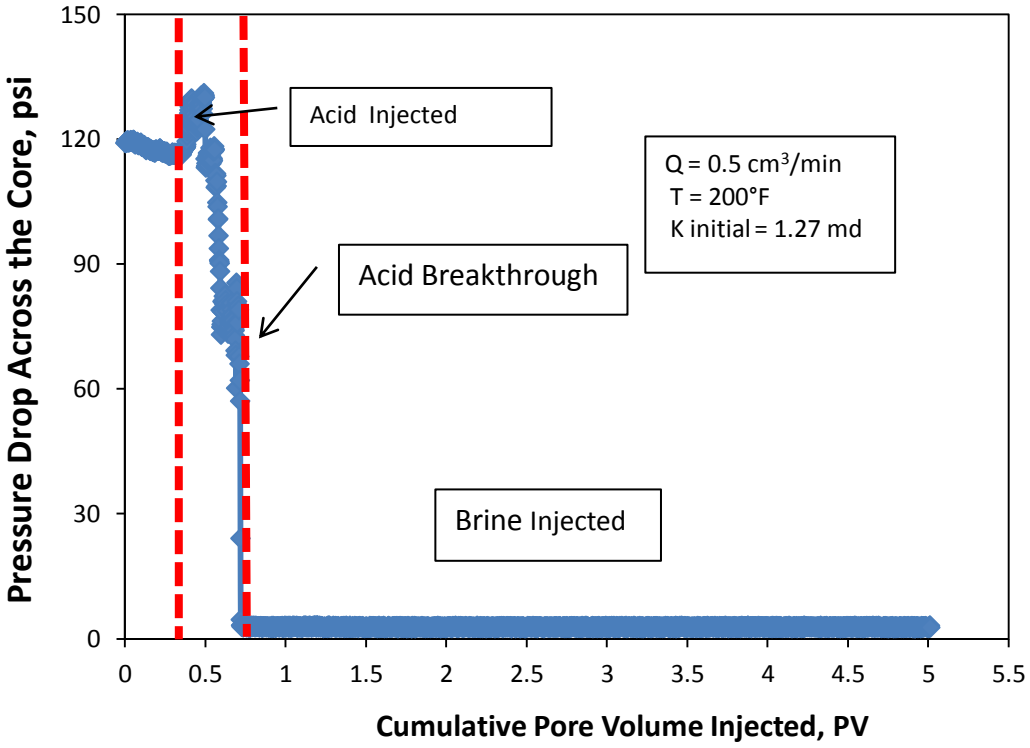

Fig. 51—Pressure drop across waterflood residual oil 6 in. core at an acid injection rate of 0.5 cm^3/min and 200°F.

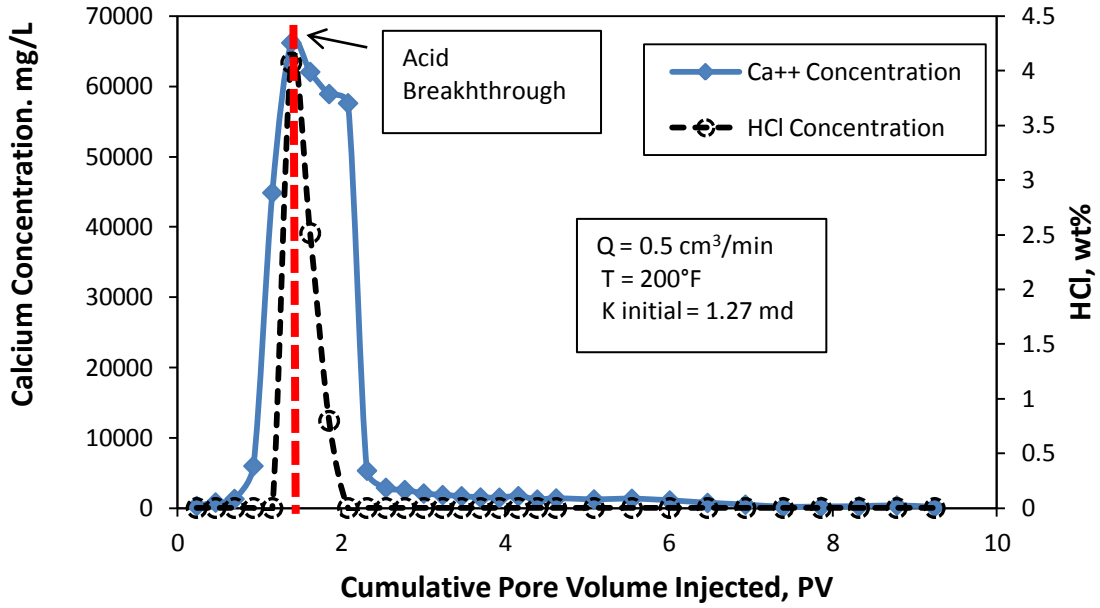

Fig. 52—Calcium and HCl concentration in the effluent samples from coreflood of waterflood residual oil 6 in. core at acid injection rate of 0.5 cm^3/min.

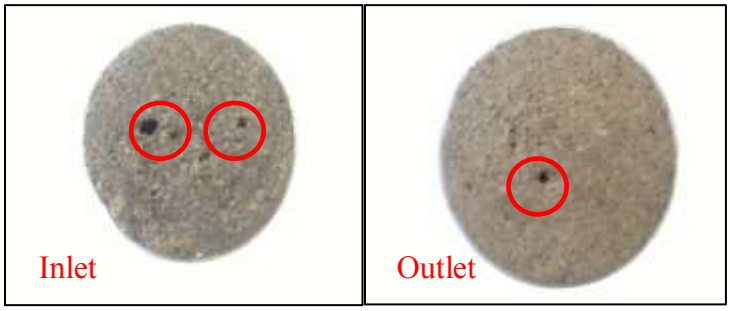

Fig. 53—Inlet and outlet face of waterflood residual oil saturated 6 in. core at 0.5 cm^3/min and 200°F.

Comparative Study

Fig. 54 shows pressure drop across all the 6 in. cores used for the comparative study. The highest pressure drop is for oil saturated cores where the acid has the greatest flow resistance due the presence of oil in the flow channels across the core. The pressure drop across the brine saturated and waterflood residual oil cores are comparable because the oil present in residual state does not hinder the flow of acid across the core.

Another interesting comparison that can be drawn is that brine saturated cores took the maximum acid pore volumes to breakthrough, followed by oil saturated cores. Waterflood residual oil cores took the least pore volumes to breakthrough. This phenomenon can be explained using the comparative calcium concentration plots for all the saturation conditions (**Fig 55**). The oil present in residual state contributes towards the fewest pore volumes of acid being used for breakthrough by acting as a buffer zone between rock and acid. The acid makes its way through the flow channels created by brine and is not spent dissolving the rock matrix. For brine saturated cores, acid mixed with brine and the relative permeability of acid through the core was unchanged, resulting in greater fluid loss to the regions surrounding the main wormhole. Consequentially, higher pore volumes of acid were consumed for creating a wormhole

Face dissolution was observed across brine saturated cores which explains the high calcium concentration in the effluent samples (**Fig. 47 & 55**). For oil saturated cores, formation of a conical wormhole accounted for higher calcium concentration in the effluent samples compared to waterflood residual oil cores. However it was not as high as brine saturated cores because of the absence of face washout.

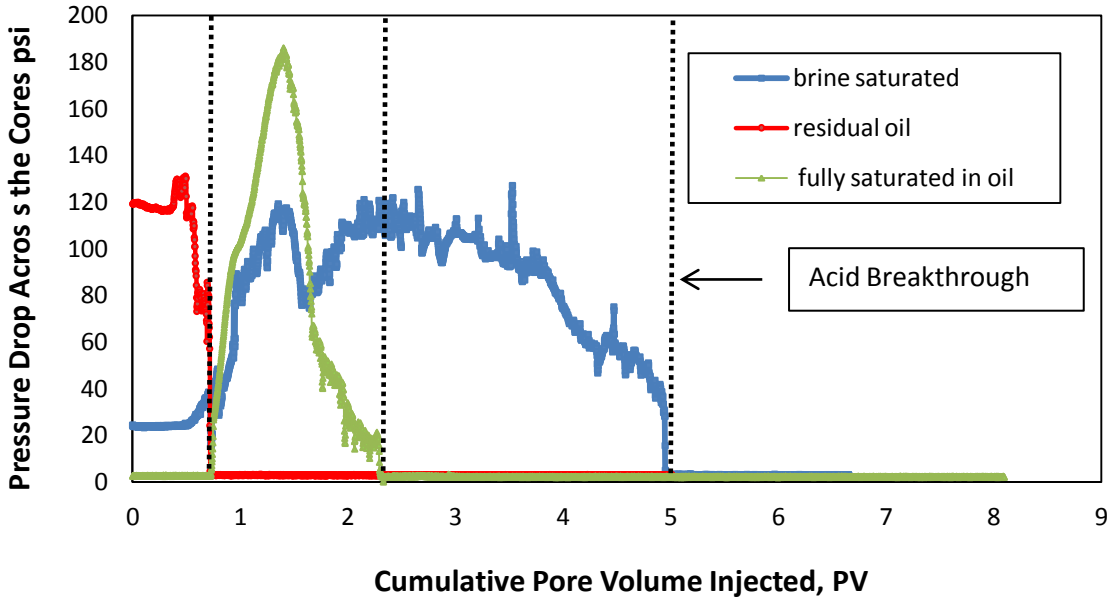

Fig. 54—Pressure drop across the cores under different saturation condition during the coreflood.

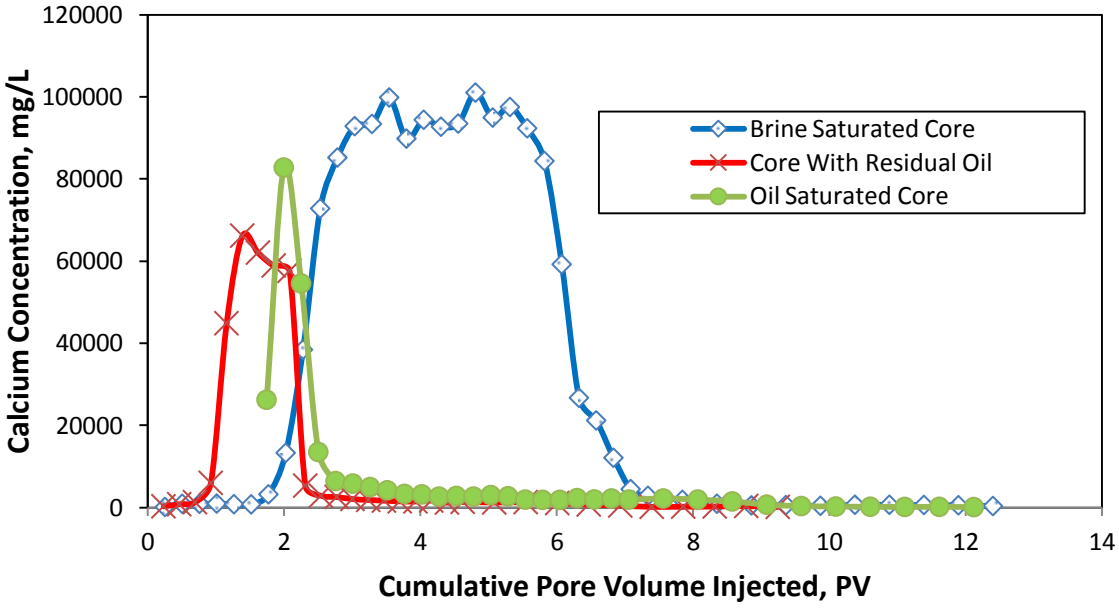

Fig. 55—Calcium concentration in the effluent samples from coreflood of cores under different saturation conditions.

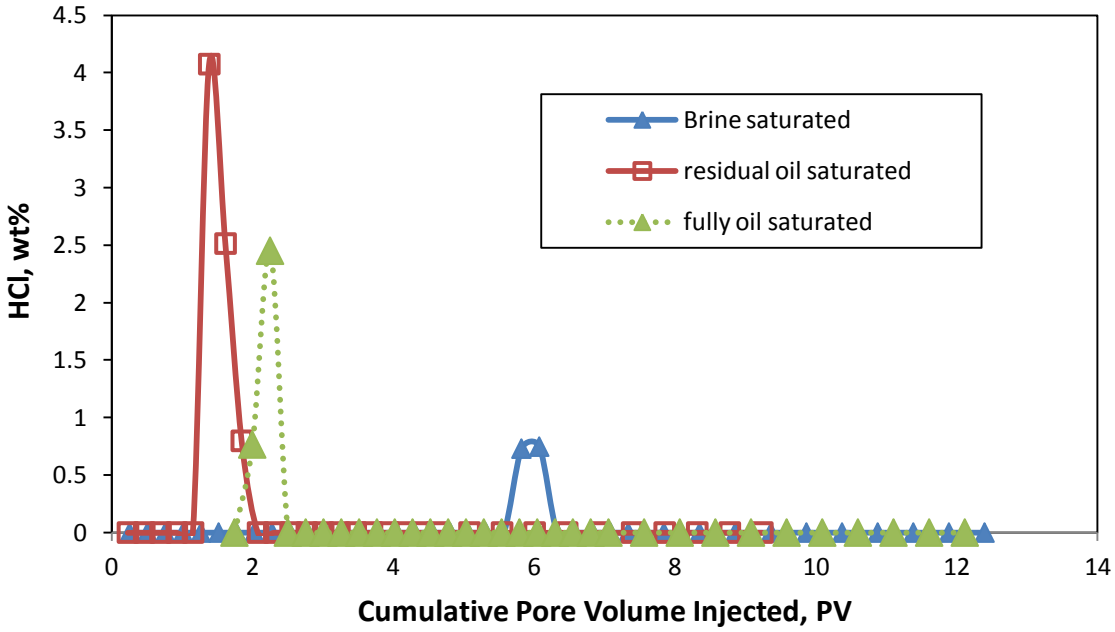

Fig. 56—HCl concentration in the effluent samples from coreflood of cores under different saturation conditions.

Fig. 56 shows that the concentrations of acid in the effluent samples are directly related to the calcium concentration profile. The highest acid concentration at breathrough was recorded for residual oil cores, indicating the least reactivity with rock whereas for brine saturated cores, the acid was consumed during face dissolution and the concentration dropped from 15 wt% to less than 1 wt%. Oil saturated cores had intermediate acid concentrations in the effluent samples.

Post Coreflood CAT Scan Images of Cores under Various Saturation Condition

2D CAT scan images of the brine saturated cores treated with regular acid at 200°F are shown in **Fig. 57.** Face dissolution was noticed initially at the core inlet face, which

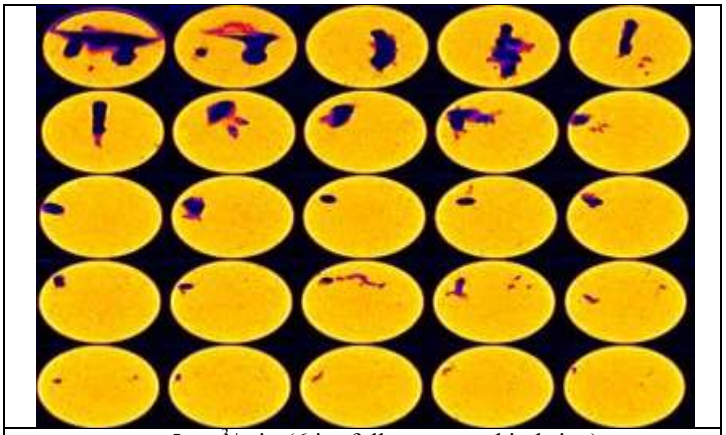

A-0.5 cm^3/min (6 in. fully saturated in brine)

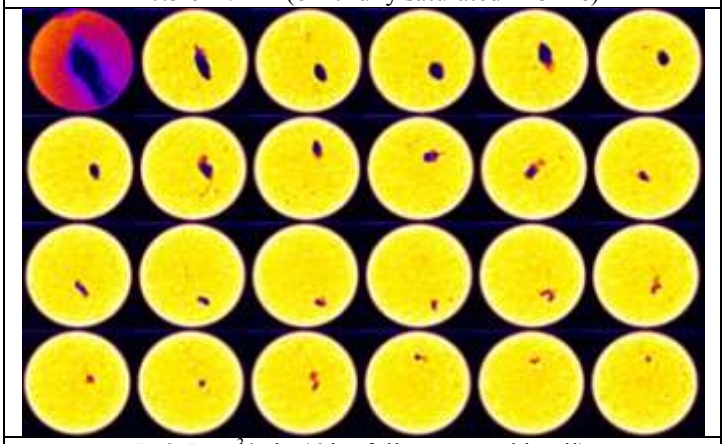

B-0.5 cm^3/min (6 in. fully saturated in oil)

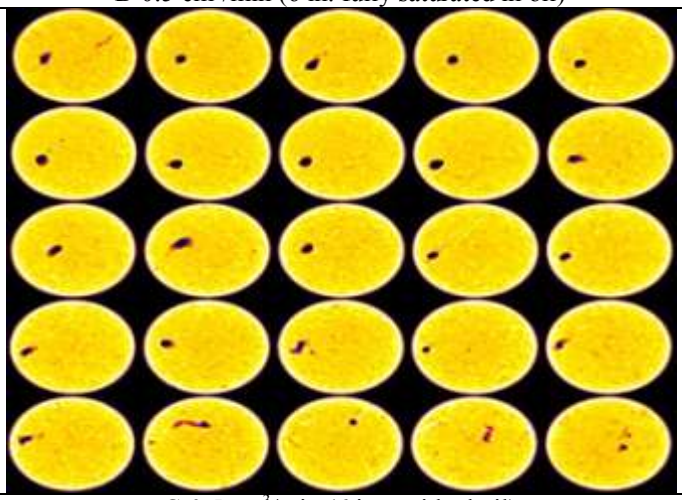

C-0.5 cm^3/min (6 in. residual oil)

Fig. 57─CAT scan images of cores under various saturation conditions after coreflood study.

accounted for the high calcium concentration in the effluent samples (**Fig. 57-A**). The diameter of the wormhole reduced as the acid propagated through the core. The wormhole created at this flow rate is non optimal.

Although there was face dissolution noticed initially for oil saturated cores (**Fig. 57-B**), the HCl acid system used propagated a wormhole with decreasing diameter as it acidized the core.

For cores with residual oil saturation, the acid system propagated wormholes with minimal branches (**Fig. 57-C**). Since the wormhole formed was more dominant than the previous two cases, calcium concentration at breakthrough was found to be the least of the three saturation conditions tested. The dissolution pattern created at low injection rate for the residual oil saturation condition resulted in the most efficient stimulation of the core.

CHAPTER VII

CONCLUSIONS AND RECOMMENDATIONS

Coreflood experiments were conducted to assess the effect of different oil saturations on acid propagation during matrix acidization of carbonate rocks. The wormhole patterns and characteristics of cores saturated in water, in oil, and with residual oil were analyzed and compared. Experimental results indicate that oil saturation does impact the wormholing characteristics of HCl while acidizing carbonate rocks. The following conclusions were drawn:

Water Saturated Cores

- At low acid injection rates, acid volume required to propagate a wormhole decreases as injection rate increases; while at high acid injection rates, acid volume required to propagate a wormhole increases slightly as injection rate increases.
- Coreflood tests for injection rates ranging from 0.5 to 20 cm^3/min showed that the optimum acid injection rate was around 10 cm^3/min, corresponding with the minimum acid pore volumes necessary for wormhole propagation across the core.
- Due to inlet face dissolution, a significant amount of calcium was measured in the effluent samples at 0.5 and 2 cm^3/min.

Waterflood Residual oil Cores

- HCl was effective in creating wormholes with minimal branches for cores with residual oil (Sor=0.4-0.5) at injection rates from 0.5 to 20 cm^3/min.
- Cores with residual oil after waterflooding showed no face dissolution at low acid injection rates.
- Compared to brine saturated and oil saturated cores, waterflood residual oil cores consumed the least acid volume to breakthrough.
- The wormholing efficiency of regular acid improved with increasing acid injection rates in the presence of residual oil, indicating that the acid should be injected at the maximum possible rate while acidizing waterflooded wells.

Oil Saturated Cores

- The severity of face dissolution for oil saturated cores was lesser at low injection rates as compared to brine saturated cores. The inlet face of the core indicates the formation of conical wormholes at low injection rates.
- Oil saturated cores did not show an optimum injection rates for breakthrough. The inlet and outlet face of the cores did not suggest the formation of a single dominant wormhole for any of the flow rates tested. However, the pore volume to breakthrough decreased with an increase in flow rate at higher injection rates.
- The decrease in acid pore volumes to breakthrough for oil saturated cores at high flow rates (20 cm^3/min) could be attributed to viscous fingering of acid through

the oil. The viscosity of crude oil was as much as 3 times that of the regular acid at 200°F.

Recommendations

Based on the above discussions, it is recommended that the saturation condition of the reservoir be studied in detail before acidizing the well. Treating oil-wet waterflood reservoir intervals requires the least amount of regular acid in comparison to brine saturated or oil saturated regions of the reservoirs. Thus, the knowledge of the saturation condition of the near wellbore area being treated helps prevent over/under designing of an acid job.

It should be noted that the current study was conducted on cores of 3 in. in length and more research work needs to be done to extend the conclusions to field scale. Some of the recommendations are as follows:

- Investigate the effect of oil saturation on acid propagation during matrix acidization of cores of different length.
- Identify the effect of different acid, the acid concentration, and temperature while acidizing oil saturated and waterflood residual oil cores.
- Comprehensive correlations accommodating all the above factors should be developed to determine the optimum acid injection rate under various reservoir conditions.

REFERENCES

Al-Mutairi, S., Al-Obied, M.A., AlYami, I. et al. 2012. Wormhole Propagation in Tar During Matrix Acidizing of Carbonate Formations. Paper presented at the SPE International Symposium and Exhibition on Formation Damage Control, Lafayette, Louisiana, USA. Society of Petroleum Engineers SPE-151560-MS. DOI: 10.2118/151560-ms.

Bazin, B. and Abdulahad, G. 1999. Experimental Investigation of Some Properties of Emulsified Acid Systems for Stimulation of Carbonate Formations. SPE 53237. This paper was presented at the Middle East Oil Show and Conference, 20-23 February, Bahrain.

Bazin, B., Roque, C. and Bouteca, M. 1995. A Laboratory Evaluation of Acid Propagation in Relation to Acid Fracturing: Results and Interpretation. Paper SPE 30085 presented at the SPE European Formation Damage Conference, The Hague, Netherlands, 15-16 May.

Bergstrom, J.M. and Miller, B.D. 1975. Results of Acid-in-Oil Emulsion Stimulations of Carbonate Formations. Presented at the Fall Meeting of the Society of Petroleum Engineers of AIME. 00005648.

Bernadiner, M.G., Thompson, K.E., and Fogler, H.S. 1992. Effect of Foams Used During Carbonate Acidizing. *SPE Production Engineering* **7** (4): 350-356. SPE-21035-PA. doi: 10.2118/21035-PA.

Buijse, M.A. 2000. Understanding Wormholing Mechanisms Can Improve Acid Treatments in Carbonate Formations. *SPE Production & Operations* **15** (3): 168-175. doi: 10.2118/65068-pa.

Buijse, M.A. and Domelen, M.S.V. 2000. Novel Application of Emulsified Acids to Matrix Stimulation of Heterogeneous Formations. SPE Production & Operations 15 (3): 208-213. 00065355.

Buijse, M.A. and Glasbergen, G. 2005. A Semi empirical Model to Calculate Wormhole Growth in Carbonate Acidizing. Paper SPE 96892 presented at the SPE Annual Technical Conference and Exhibition, Dallas, Texas, 10/09/2005. doi:10.2118/96892-MS.

Cole-Palmer.Inc.,2013.Titrators. http://www.coleparmer.com/Product/Thermo_Scientific_Orion_950_Titrator_w_printer_110_120_VAC/EW-24909-10. Downloaded 8 August 2013.

Crowe, C.W. and Miller, B.D. 1974. New, Low-Viscosity Acid-in-Oil Emulsions Provide High Degree of Retardation at High Temperature. Presented at the SPE Rocky Mountain Regional Meeting. 00004937.

Daccord, G., Lenormand, R. and Liétard, O. 1993. Chemical Dissolution of a Porous Medium by a Reactive Fluid. *Chemical Engineering Science* **48**(1): 169–186.

Daccord, G., Touboul, E., and Lenormand, R. 1989. Carbonate Acidizing: Toward a Quantitative Model of the Wormholing Phenomenon. *SPE Production Engineering* **4** (1): 63-68. doi: 10.2118/16887-pa.

Economides, M.J. and Kenneth, G.N. 2000. *Reservoir Stimulation*. 2nd edition. Houston, Texas: Gulf Publishing Company.

Economides M. J., Hill A. D., Economides C. E., C. *Petroleum Production System*, 400. 1993. Upper Saddle River, New Jersey: Prentice Hall, Inc.

Foshee, W.C. and Hurst, R.E. 1965. Improvement of Well Stimulation Fluids by Including a Gas Phase. Journal of Petroleum Technology. Volume 17, Number 7. pp:768-772. DOI: 10.2118/803-PA

Fredd, C.N. 2000. *Reservoir Stimulation: Advances in Understanding and Predicting Wormhole Formation*. 3rd edition, Englewood Cliffs, New Jersey: Prentice Hall.

Fredd, C.N. and Fogler, H.S. 1998a. Alternative Stimulation Fluids and Their Impact on Carbonate Acidizing. *SPE Journal* **13**(1): 34-41.

Fredd, C.N. and Fogler, H.S. 1998b. Influence of Transport and Reaction on Wormhole Formation in Porous Media. *AIChE J.* **44**(9):1933–1949.

Fredd, C.N. and Fogler, H.S. 1998c. The Influence of Chelating Agents on the Kinetics of Calcite Dissolution. *Journal of Colloid and Interface Science*, **204** (1): 187-197. doi**:**10.1289/ehp.

Fredd, C.N. and Fogler, H.S. 1999. Optimum Conditions for Wormhole Formation in Carbonate Porous Media: Influence of Transport and Reaction. *SPE Journal* **4** (3): 196-205. doi: 10.2118/56995-pa.

Frick, T.P., Mostofizadeh, B., and Economides, M.J. 1994. Analysis of Radial Core Experiments for Hydrochloric Acid Interaction with Limestones. Paper SPE 27402 presented at the SPE International Symposium on Formation Damage Control, Lafayette, Louisiana, 7-10 February.

Furui, K., Burton, R.C., Burkhead, D.W., Abdelmalek, N.A., Hill, A.D. et al. 2010. A Comprehensive Model of High-Rate Matrix Acid Stimulation for Long Horizontal Wells in Carbonate Reservoirs. Paper SPE 134265-MS presented at the SPE Annual Technical Conference and Exhibition, Florence, Italy, 09/19/2010. doi: 10.2118/134265-ms.

Gdanski, R. 1999. A Fundamentally New Model of Acid Wormholing in Carbonates.Paper SPE 54719 presented at the SPE European Formation Damage Conference, The Hague, Netherlands, 05/31/1999. doi: 10.2118/54719-ms.

Gomaa, A.M. and Nasr-El-Din, H. 2011. Effect of Residual Oil Saturation on the Propagation of Regular, Gelled, and in-Situ Gelled Acids inside Carbonate Formations. Paper presented at the SPE European Formation Damage Conference, Noordwijk, The Netherlands. Society of Petroleum Engineers SPE-143643-MS. DOI: 10.2118/143643-ms.

Guidry, G.S., Ruiz, G.A., and Saxon, A. 1989. Sxe/N2 Matrix Acidizing. Presented at the Middle East Oil Show. SPE 17951.

He., J, Mohamed, I. M., and Nasr-El-Din, H.: "Mixing Hydrochloric Acid and Seawater for Matrix Acidizing: Is It a Good Practice?", SPE 143855 presented at the SPE European Formation Damage Conference, Noordwijk, The Netherlands, June 7-10,2011.

Hoefner, M.L. and Fogler, H.S. 1988. Pore Evolution and Channel Formation During Flow and Reaction in Porous Media. *AIChE J.* **34**(1): 45–54.

Hoefner, M.L. and Fogler, H.S. 1987. Role of Acid Diffusion in Matrix Acidizing of Carbonates. *SPE Journal of Petroleum Technology* **39** (2): 203-208. doi:10.2118/13564-pa.

Hoefner, M.L. and Fogler, H.S. 1985. Effective Matrix Acidizing in Carbonates Using Micro emulsions. *Chemical Engineering Progress* (May), **81**: 40-44.doi: 10.1016/ j.petrol.2006. 08. 005.

Huang, T., McElfresh, M.P., and Gabrysch, A.D. 2003. Carbonate Acidizing Fluids at High Temperatures: Acetic Acid, Chelating Agents or Long-Chained Carboxylic Acids. Paper SPE 82268 presented at the SPE European Formation Damage Conference, The Hague, The Netherlands, 13-14 May. SPE 82268-MS.

Huang, T., Hill, A.D., and Schechter, R.S. 2000. Reaction Rate and Fluid Loss: The Keys to Wormhole Initiation and Propagation in Carbonate Acidizing. *SPE Journal* **5** (3): 287-292. doi: 10.2118/65400-pa.

Huang, T., Zhu, D., and Hill, A.D. 1999. Prediction of Wormhole Population Density in Carbonate Matrix Acidizing. Paper SPE 54723 presented at the SPE European Formation Damage Conference, The Hague, Netherlands, 05/31/1999. doi:10.2118/54723-ms.

Huang, T., Hill, A.D. and Schechter, R.S. 1997. Reaction Rate and Fluid Loss: The Keys to Wormhole Initiation and Propagation in Carbonate Acidizing. Paper SPE 37312 presented at the SPE International Symposium on Oilfield Chemistry, Houston, Texas, 18-21 February.

Izeg, O. and Demiral, B. 2005. CO_2 Injection in Carbonates. Paper SPE 93773 presented at the SPE Western Regional Meeting, Irvine, CA, 30 March-1 April. doi: 10. 2118/93773-MS.

Lund, K., Fogler, H.S., McCune, C.C., and Ault, J.W. 1975. Acidization II. The Dissolution of Calcite in Hydrochloric Acid. *Chemical Engineering Science* **30** (8): 825-835.

Mahmoud, M.A., Nasr-El-Din, H.A., DeWolf, C. et al. 2011. Effect of Reservoir Fluid Type on the Stimulation of Carbonate Cores Using Chelating Agents. Paper presented at the Brasil Offshore, Macaé, Brazil. Society of Petroleum Engineers SPE-143086-MS. DOI: 10.2118/143086-ms.

Mostofizadeh, B. and Economides, M.J. 1994. Optimum Injection Rate from Radial Acidizing Experiments. Paper SPE 28547 presented at the SPE Annual Technical Conference and Exhibition, New Orleans, Louisiana, 25-28 September.

Navarrete, R.C., Miller, M.J., and Gordon, J.E. 1998a. Laboratory and Theoretical Studies for Acid Fracture Stimulation Optimization. Presented at the SPE Permian Basin Oil and Gas Recovery Conference. 00039776.

Navarrete, R.C., Holms, B.A., McConnell, S.B. et al. 1998b. Emulsified Acid Enhances Well Production in High-Temperature Carbonate Formations. Presented at the European Petroleum Conference. 00050612.

Nevans, J.W., T. Blasingame, L.Doublet, G. Freeman, J Callard, D. Moore, Davies, R. Vessell, B. Pregger. 1996. Annual report for U.S.Department of Energy office of Fossil Energy. Application of Integrated Reservoir Management and Reservoir Characterization to Optimize Infill Drillings.

Perkin Elmers. Inc.,2013. Spectrometers http://shop.perkinelmer.com/content/relatedmaterials/productnotes/prd_optima7000d .pdf Downloaded 14 April 2013.

Peters, F.W. and Saxon, A. 1989. Nitrified Emulsion Provides Dramatic Improvements in Live Acid Penetration. Paper presented at the SPE Asia-Pacific Conference, Sydney, Australia. 1989 Copyright 1989, Society of Petroleum Engineers, Inc. 00019496. DOI: 10.2118/19496-ms.

Robert, J.A. and Crowe, C.W. 2000. *Reservoir Stimulation: Carbonate Acidizing Design*. 3rd edition, Englewood Cliffs, New Jersey: Prentice Hall.

Sayed, M.A.I., Assem, A.I., and Nasr-El-Din, H.A. 2012. Effect of Presence of Crude Oil on the Performance of Emulsified Acids. Paper presented at the North Africa Technical Conference and Exhibition, Cairo, Egypt. Society of Petroleum Engineers SPE-152844-MS. DOI: 10.2118/152844-ms.

Schechter, R.S. and Gidley, J.L. 1969. The Change in Pore Size Distribution from Surface Reactions in Porous Media. *AIChE Journal* **15** (3): 339-350. doi:10.1002/aic.690150309.

Shukla, S., Zhu, D. and Hill, A.D. 2006. The Effect of Phase Saturation Conditions on Wormhole Propagation in Carbonate Acidizing. SPE Journal. Volume 11, Number 3. Pp. 273-281. DOI: 10.2118/82273-PA.

Teledyne Isco, Inc. 2013. D Series Pump http://www.isco.com/products/products3.asp?PL=1051020. Downloaded 14 April 2013.

Wang, Y., Hill, A.D. and Schechter, R.S. 1993. The Optimum Injection Rate for Matrix Acidizing of Carbonate Formations. Paper SPE 26578 presented at the SPE Annual Technical Conference and Exhibition, Houston, Texas. 3-6 October.

Williams, B.B., Gidley, J.L., and Schechter, R.S. 1979. *Acidizing Fundamentals.* New York: Society of Petroleum Engineers of AIME.